

Satellite Based Intertidal-Zone Mapping from Sentinel-1&2

Sluttrapport: Fjernmålingsbasert kartlegging og overvåking av tidevannssonen

Mars 2020

Jörg Haarpaintner, Corine Davids



Project title:	Fjernmålingsbasert kartlegging og overvåking av tidevannssonen.
Project number:	101800
Institution:	NORCE – Norwegian Research Centre AS
Client/s:	Miljødirektoratet (MD) Project: M-1646 2020 Satellite Based Intertidal-Zone Mapping from Sentinel-1&2 Contact person: Tomas Holmern
Classification:	Public
Report no.:	2-2020 (NORCE KLIMA)
ISBN:	978-82-8408-070-3
Number of pages:	57
Publication month:	March 2020
Citation:	Haarpaintner, J. & C. Davids. Satellite Based Intertidal-Zone Mapping from Sentinel-1&2. Final Report, NORCE Klima Report nr. 2-2020. March 2020.
Captions and credits:	Contains modified Copernicus Sentinel-1&2 data (2017-2018), processed by NORCE

Summary:

The report describes developed methods and results based on radar and optical high resolution (10-20m) satellite imagery from Sentinel-1 C-band synthetic aperture radars (C-SAR) S1A and S1B and Sentinel-2 MultiSpectral Instruments (MSI) S2A and S2B from the European Copernicus Program to map the intertidal zone in Trondheimsfjorden, Norway, with the aim to extend it nationally.

Revisions

Rev.	Date	Author	Checked by	Approved by	Reason for revision
V 0.0	10.12.2019	J. Haarpaintner	C. Davids		Foreløpig rapport
v.0	17.02.2020	J. Haarpaintner	C. Davids		Draft
v.1	04.03.2020	J. Haarpaintner	C. Davids		Revision after MD comments
v.1.1	18.03.2020	J. Haarpaintner	C. Davids		ISBN nr & typos

Tromsø, 18.03.2020

Jörg Haarpaintner
Project manager

Corine Davids
Quality assurance

Tomas Holmern
Contact person at MD

Disclaimer – limitation of liability

The authors assume no responsibility or liability for any errors or omissions in the content of this research report. The information contained in this report is provided "as is", based on their best knowledge and effort during the work of the project with no guarantees of completeness, and accuracy.

Preface

In 2019, the Norwegian Environment Agency issued a call for tender to map and monitor the intertidal zone of Norway with free remote sensing data. In a first phase, the winning tender should develop methods and algorithms that are able to map the intertidal zone area, distinguish between different types and environmental parameters of the intertidal zones in order to be able to do this operationally on a periodic basis. The methods should be demonstrated on Trondheimsfjord. The continuation in the following phases should then lead to a processing system that leads to a national intertidal zone map, as well as the potential to detect changes in this area.

NORCE – the Norwegian Research Centre AS successfully responded to the tender proposing to develop methods focusing on the use of Sentinel-1 and Sentinel-2 of the European Copernicus Program. This is the final report of phase 1 under contract M-1646|2020.

Table of Contents

Disclaimer – limitation of liability	2
Preface	3
List of figures	6
List of tables	8
Abstract	9
1. Background	11
1.1 Mapping of coastal ecosystems.....	11
1.2 Tides and intertidal zones	12
1.3 Intertidal zone ecosystems.....	14
1.4 Project Objective.....	15
2. Data	16
2.1 Demonstration Site - Trondheimsfjorden	16
2.2 Satellite data	16
2.2.1 Sentinel-1	16
2.2.2 Sentinel-2	19
2.3 Aerial and ground reference data.....	20
2.3.1 Aerial photos from Norgebilder.no	20
2.3.2 Vector data from “Naturbase”	21
2.3.3 In-situ data	21
3. Methods	22
3.1 Pre-processing.....	22
3.1.1 Sentinel-1 CSAR	22
3.1.2 Sentinel-2	22
3.2 Intertidal-zone mapping	23

3.2.1	Intertidal-zone area mapping with Sentinel-1 CSAR	23
3.2.2	Intertidal zone area and type mapping with Sentinel-2	26
3.2.3	Intertidal zone type mapping with Sentinel-1	30
3.2.4	Use of aerial data	30
3.3	Mapping of atmospheric exposure (“Tørrleggingsvarighet”) with SAR	31
3.4	Mapping of intertidal zone changes	34
4.	Results	35
4.1	Intertidal Zone Area Mapping	35
4.1.1	Intertidal Zone Area Mapping with Sentinel-1	35
4.1.2	Mapping intertidal zones using Sentinel-2	38
4.2	Intertidal Zone Type Mapping	39
4.2.1	Mapping intertidal ecosystems using Sentinel-2	39
4.2.2	Intertidal Zone Type from Sentinel-1	41
4.3	Mapping of atmospheric exposure with Sentinel-1	43
4.4	Mapping changes in the intertidal zone.	45
5.	Accuracy Assessment	46
5.1	Field validation	46
5.2	Inter-comparison between Sentinel-1 and Sentinel-2 results.....	49
6.	Conclusion	50
7.	Recommendations	51
7.1	National Intertidal-zone mapping.....	51
7.2	Accuracy assessment.....	52
7.3	Proposal for nationwide mapping	53
8.	Project limitation	54
9.	Acknowledgments	54
10.	References	54

List of figures

Figure 1. Illustration of tidal terms (Tide Terms by User: Ulamm / Wikimedia Commons / CC-BY-SA-3.0).....13

Figure 2. Tidal range variations in Tromsø, July 2019. Tidal data from Se Havnivå (<http://www.kartverket.no>).....13

Figure 3. Trondheimsfjorden (@GoogleMaps).....16

Figure 4. Sentinel-1 paths and coverage of the demonstration area Trondheimsfjorden (yellow rectangle).18

Figure 5. Low percentile (minimum, left) and high percentile (maximum, right) backscatter mosaics over Trondheimsfjorden. RGB=[VV,VH,NDI].23

Figure 6. Median value (50 percentile value) VV and VH backscatter histogram over the Trondheimsfjorden area from Sentinel-1 2018 data. The left mode represents backscatter over water and the right mode, backscatter over land for both polarizations, VV and VH.24

Figure 7. Tidal chart for Trondheim for August 2019 with the Sentinel-1 overpasses indicated with black bars.24

Figure 8. 2 percentile, median value (50 percentile) and 98 percentile Sentinel-1 VV and VH image histograms over the Trondheimsfjorden area from 2018 data.25

Figure 9. Legend of the Intertidal Zone Area products.....26

Figure 10. Processing workflow used for Sentinel-2.27

Figure 11. Number of images used in the analysis after cloud masking.28

Figure 12. Example of training polygons in areas around Tautra (left) and Grandefjære (right).29

Figure 13. Legend of Intertidal Zone Type maps.30

Figure 14. VV Backscatter distribution of percentile images at 2%, 5%, 25%, 50%, 75%, 95% and 98 % percentile.....32

Figure 15. VH Backscatter distribution of percentile images at 2%, 5%, 25%, 50%, 75%, 95% and 98 % percentile.....32

Figure 16. Land water threshold vs percentile image for VV and VH polarizations.33

Figure 17. Legend of Intertidal Zone Atmospheric Exposure maps.....33

Figure 18. Final Sentinel-1 based Intertidal zone area (red) product in Trondheimsfjorden in UTM zone 32N35

Figure 19. Intertidal zones in red detected by thresholding low and high backscatter percentiles. 36

Figure 20. Zoom-ins of the intertidal zone results around Grandefjære/Storfosna and the northeast of Trondheimsfjorden.....36

Figure 21. Detected intertidal zone area (red) superimposed on an aerial image from Storfosna. .37

Figure 22. (Left) Minimum and (middle) maximum Sentinel-1 backscatter mosaics and (right) the detected intertidal zone area (red line) superimposed on an aerial image over Tautra.....37

Figure 23. Intertidal zones indicated in red, plotted on an image showing the tndvi interval mean 10-90.38

Figure 24. Detail of the extent of the intertidal zone of the Grandefjære site, as mapped by Sentinel-2 analysis. On the left, the intertidal zone is plotted in red on an aerial photo, with the bløtbunn (mudflat) vector data from Naturbase indicated by a yellow line. On the right, aerial photos at low tide (2010) with the bløtbunn dataset from Naturbase.39

Figure 25. Details within the intertidal zone of the Grandefjære Ramsar site. Left: 7 classes identified within, and adjacent to, the intertidal zone, plotted on an aerial photo. Only the area in the coastal mask is classified. Right: aerial photo with lowest tidal level available (2010) from Norge i Bilder, overlain by the bløtbunn vector data in yellow, for visual comparison.39

Figure 26. Details within the intertidal zone of the Tautra Ramsar site. Left: 7 classes identified within, and adjacent to, the intertidal zone, GMM segmentation. Right: aerial photo with lowest tidal level available (2009) from Norge-i-Bilder, overlain by the bløtbunn vector data in yellow, for visual comparison.40

Figure 27. Final intertidal zone type based on Sentinel-1 2017-2018 data of Trondheimsfjorden using an MLH classification with all percentile images.....41

Figure 28. Zoom-in on Grandefjære of the type classification using MLH on (a) all percentile images, (b) on the 98% percentile VV and VH images, and using NN on (c) all percentile images, (d) on the 98% percentile VV and VH images. (e) is the aerial image as reference.42

Figure 29. Final intertidal zone atmospheric exposure product based on Sentinel-1 2017-2018 data of Trondheimsfjorden.....43

Figure 30. Zoom-in of the ITZ_AtMExp around Grandefjære and Storfosna at the exit of Trondheimsfjorden in the west.44

Figure 31. Zoom-in of the ITZ_AtMExp around (a) Tautra island and (b) Kausmofjære/Verdal.44

Figure 32. Detected establishment of a new sand mine at Småtta close to Vigtil. (Upper left) aerial photo from 16 Sep 2014, (Upper right) aerial photo from 17 May 2019, (Lower left) change detected from S1 between 2017 and 2018, (lower right) S1 averaged mosaic 2018.45

Figure 33. Detected changes in the harbour of Verdal from 2017 to 2018 by thresholding the difference of the 95% percentile images from both years. The aerial images date from 30 June 2017 and 17 May 2019.45

Figure 34. Field site Lille Grindøya close to Tromsø. The image composite shows a combination of VH percentiles in RGB=[95, 50, 5]. The intertidal zone is in red. The white line shows the GPS track from walking along the waterline. The green line shows the Contour line of -20.5dB of the 95%ile.46

Figure 35. Zoom-in of Figure 34 on Lille Grindøy. The green line shows the GPS track from walking along the waterline around high tide on 19 July 2019. The red line shows the maximum extent of the intertidal zone area measured with the proposed method with Sentinel-1.47

Figure 36. Zoom-in of Figure 34 on Lille Grindøya. The coloured lines show line of different percentages of atmospheric exposure. line shows the GPS track from walking along the waterline. The green line shows the Contour line of -20.5dB of the 95%ile.....47

Figure 37. Applying different thresholds on the 95-percentile image. Threshold var from -21 dB to -16 dB. The orange line is a threshold of -20.5dB.....48

Figure 38. Thresholding of the 5% percentile for the high-tide water line, i.e. land detection with VH backscatter thresholds varying from -25dB to -19dB48

Figure 39. Inter-comparison between S2 (left panels) and S1 (right panels) results around Grandefjære (upper panels) and Tautra (lower panels)49

List of tables

Table 1. Sentinel-1 path numbers off a 12-day cycle (starting 01.08.2019) covering Trondheimsfjorden specifying the satellite, path and direction.	18
Table 2. Band specifications Sentinel-2 (https://sentinel.esa.int/web/sentinel/user-guides/sentinel-2-msi/resolutions/radiometric).....	19
Table 3. Land-water threshold values for VV and VH backscatter for the percentile images of 2%, 5%, 25%, 50%, 75%, 95% and 98 % percentile for each year 2017 and 2018.	31

Abstract

The goal of this study is to develop methods based on radar and optical high resolution (10-20m) satellite imagery from Sentinel-1 C-band synthetic aperture radars (C-SAR) S1A and S1B and Sentinel-2 MultiSpectral Instruments (MSI) S2A and S2B from the European Copernicus Program to map the intertidal zone in Trondheimsfjorden, Norway, with the aim to extend it nationally.

The overall approach is to use long dense times series of satellite acquisitions and the fact that the frequency of satellite acquisition is different than the tidal period of ~12.25h, to ensure acquisitions of the full range of tidal cycle levels. Both sensors CSAR and MSI can distinguish between water covered areas and land, but as SAR is independent of cloud cover and sunlight, it can sample the tidal levels to a much higher rate than optical sensors that need cloud free conditions to observe the earth's surface.

All S1 (A&B) from 2017 and 2018 data were processed and statistically analyzed. At the latitude of Trondheimsfjorden, each pixel is covered nearly on a daily basis by 240 to 360 acquisitions per year. Percentile values of the radar backscatter in co- and cross polarization, VV and VH, were extracted for each pixel at 2%, 5%, 25%, 50%, 75%, 95% and 98% percentiles and represented as percentile mosaics over the study area. As water and land can be separated by simple thresholding, pixels in the intertidal zone will be then classified as land or water dependent on the percentile image. Specific thresholds for each percentile are extracted from the backscatter distribution using the minimum between a water and a land mode. Each threshold contour line corresponds then directly to a certain tidal level. The water line of the 2% percentile will correspond to the (near-) highest tide and the 98% percentile to the near-lowest tide waterline. The area in between defines the intertidal zone area. Extracted water lines at other percentile values correspond to different atmospheric exposure levels ("Tørrleggingsvarighet") in the intertidal zone.

Similar to the S1 approach, the methodology used for the analysis of Sentinel-2 data for the purpose of mapping tidal zones uses statistical parameters calculated from time series of several vegetation and water indices and is inspired by the methodology presented by Murray et al. (2019). Instead of thresholding, unsupervised and supervised classifiers have been applied to classify into permanent water, land, mudflat, sandy/gravel beach, rocky shoreline, seaweed, and shallow water. A total of 85 training polygons identifying these 7 classes were created for this purpose from aerial mosaics. Due to cloud cover and dark winter months in Norway, the number of acquisitions however is reduced to 15 to 73 times per pixel/year for 2018. Still, the intertidal zone area detected by S2 corresponds well and is in general only slightly smaller than the one detected with S1. Suspended sediments from river outflows can locally cause misclassification and will require more specific training data.

The training polygons extracted from aerial images were also used to perform a multivariate maximum likelihood and a neural network classification on the full set of S1 percentile images as well as only using the 95% percentile VV and VH mosaics, limited to the detected intertidal zone area. Overall, dominant classified areas of mudflats and seaweed areas agree well with the S2 type products. Training polygons of the other classes were to a vast extent outside of the detected intertidal zone area of S1 and therefore underrepresented.

Aerial images from norgebilder.no turned out not to be suitable to map the intertidal zone for several reasons on a large scale: the aerial mosaics are not consistently acquired, neither in space, nor in quality, nor in resolution, nor in similar light condition, and nor in time, which makes it nearly impossible to map the intertidal zone on a national scale; only acquisition dates are available for the mosaics and not exact acquisition times which makes it difficult to define the tidal level for interpretation; observations are too few to ensure acquisitions at highest and lowest tides; and water line are not clearly visible and shallow water area can be easily misinterpreted as intertidal zones. This limits also the possibility to use the aerial image data base directly for validation. Field data collection is therefore considered crucial to validate the mapping results from the S1 and S2 in regard to the intertidal zone area and atmospheric exposure rate, but also to learn better how to identify different types of the intertidal zone from aerial images, such as mudflats and sand.

A one to two-week field campaign in Trondheimsfjorden and some shorter field visits in southern and northern Norway are therefore suggested for the next phase of this project. A validation of both S1 and S2 results individually is also necessary in order to combine these two sensor types in the future. A one day field campaign around Lille Grindøya in Troms, also showed some additional challenges; the water line is rarely a clear line in shallow waters and small topographic features like small rocks, seaweed at the surface in shallow water and sand banks are challenging examples for a simple intertidal zone definition of surfaces being covered by water at high tides.

The study shows however clearly that both S1 and S2 are well suited to map the intertidal zone when using very long time series. Results were beyond expectation. S1 probably performs better to detect the maximum extent of the intertidal zone because of the higher temporal sampling rate. S1 has therefore also the possibility to better map the rate of atmospheric exposure inside the intertidal zone. We assume that S2 can better distinguish between different types of intertidal zones. Results from both S1 and S2 individually however correspond well with each other in regard to both, the intertidal zone area and dominant intertidal zone types, like mudflats and seaweed areas. The results and these assumptions however still need to be validated in more detail and confirmed with field observation.

The methods applied here should in theory also work on a national scale. Some clear challenges though have to be resolved. The huge amount of data makes it necessary to take the methods to the data in the internet cloud, especially if multi-year processing is considered. Different options are available and need to be compared. Similar S1 processing has been successfully tested in another project on CreoDIAS, one of the Copernicus Data and Information Access Services The analysis based on Sentinel-2 data was implemented in Google Earth Engine, which facilitates the handling of time series and large data quantities, and can in theory be extended directly to a national scale. However, different lightning and climate condition in North and South Norway, with the presence of for example fjord ice in the North needs to be considered and may require some regional adaption. In general, experience from other projects have shown that extending regional studies to a larger area often bring some unexpected challenges.

1. Background

1.1 Mapping of coastal ecosystems

The report 'Global Assessment on Biodiversity and Ecosystem Services', published by IPBES (IPBES, 2019), concludes that coastal ecosystems are vulnerable for strong pressures from both changes in land use (e.g. new constructions, habitat destruction, coastal erosion, contamination), changes in marine use (e.g. aquaculture), and climate change. Coastal ecosystems deliver important ecosystem services, such as coastal protection, coast stabilisation, recreation, and food production (Murray et al., 2018). In addition, tidal zones, in particular mudflats, can have a large biodiversity and are often important areas for shorebirds and seabirds. The tidal zone is defined as the area which is exposed to air at low tide and covered by water at high tide. Tidal zones include, for example, mudflats, sandy beaches, rocky beaches and steep cliffs. With respect to the 'Naturtyper i Norge' (NiN) system, the main types that occur in tidal zones are: M3 fast fjærelte-bunn, M4 eufotisk marin sedimentbunn, and M8 helofytt-saltvannssump.

Norway has a long coastline with locally extensive tidal zones. Traditional mapping and monitoring of these tidal zones is a challenge and use of remote sensing data can therefore be a good solution for both mapping and monitoring. Tidal zones are highly dynamic and one of the challenges with the use of remote sensing data is therefore the time of acquisition relative to the tidal state. Additional challenges include the high spatial resolution needed for mapping, the separability of the spectral properties of the different zones and bottom conditions, and regular cloud cover. As a result of the increased availability of satellite images in recent years, there has been a focus on national and global level satellite-based mapping of wetlands and coastal areas (Davidson et al., 2019; Murray et al., 2018; Rebelo et al., 2018). For example, EU project Satellite-based Wetland Observation Service (SWOS) developed tools to map wetlands based on both radar and optical satellite data (SWOS toolbox). Based on time series of Landsat images, Murray et al. (2019) produced a map showing the global extent (between +/- 60° latitude) of tidal zones.

There are many types of remote sensing data: from different platforms, such as satellite, aerial or drone; and with different sensors, such as radar (SAR), optical, lidar, or thermal. Historically, optical aerial and satellite data has been the most important for the mapping of vegetation and landscape types. In particular Landsat satellites, which have optical bands in the visible, near infrared and shortwave infrared part of the spectrum, with 30 m spatial resolution, have been used extensively in land use and vegetation mapping. The Landsat satellite image archive goes back to 1972 and is now freely available and therefore particularly useful for the mapping of changes. The first Sentinel satellites from the European Copernicus program were launched in 2014/2015; today, the program includes Sentinel-1A/B (S1), Sentinel 2A/B (S2) and Sentinel-3 (S3). S1 are two C-band radar satellites (SAR = synthetic aperture radar) with 20 m spatial resolution; S2 are two optical satellites with bands similar to Landsat, but with 10/20 m spatial resolution. Since there are two radar and two optical satellites, images are acquired over Norway nearly every day for both radar and optical satellites; this produces large quantities of data and gives the possibility for dense time series and high temporal resolution.

Optical remote sensing measures the reflection of solar irradiation on surfaces; as different surfaces, or objects, have different spectral properties, the spectral signatures (reflection in the different parts of the spectrum) can be used to identify and separate different surfaces as long as

the spectral signatures are separable. Optical remote sensing is dependent on cloud free conditions, which in Norway significantly influences the amount of data that can be used. Radar data, however, is independent of cloud cover or darkness and is acquired all year round. Radar data is sensitive to surface roughness and moisture and is therefore particularly useful for the mapping of soil moisture, water surfaces, surface roughness and changes over time.

Tides are caused by the gravitational effects of the sun and moon and the rotation of the earth. Tidal water levels do, however, not only depend on the position of the sun and moon, but also on the bathymetry, coastline, fjords and straits, and can therefore also vary geographically at relatively short distances. This means that a single acquisition of satellite, aerial photo or LiDAR data does not capture the same tidal level across the whole area. Murray et al. (2019) calculated statistical parameters from time series of a number of vegetation and water indices, and used these in combination with bathymetric and topographic data, expert knowledge to create a training/validation dataset and machine learning techniques (random forest) to differentiate between permanent water, tidal zones, and other (land, including vegetated tidal zones). In order to map the extent of tidal zones as accurately as possible, it is necessary to capture both the highest and lowest water levels. As satellite data is acquired at fixed times, which do not necessarily coincide with maximum/minimum tides, long time series of satellite data are required to capture the full tidal range.

S1 SAR satellite data is expected to be ideal for the mapping and monitoring of the extent of tidal zones and changes on a national scale, while S2 optical satellite data is expected to perform better at distinguishing variations and land types within the tidal zones. As SAR and optical satellite sensors observe different properties of the terrain, identifying their strengths and weaknesses with respect to the mapping of intertidal zones would help to develop methods to combine the datasets and improve the final products. The Sentinel satellites have a spatial resolution of 10-20 m. For more detailed mapping of the intertidal zones, aerial photographs may be used. However, the available aerial photographs are limited to about one dataset per year, and the quality varies between the years. In addition, the timing relative to the tidal cycle is unknown and unlikely to coincide with the lowest tide. In addition to the mapping of the extent of intertidal zones and identification of different landscape types within, there is a need to monitor changes in the intertidal zones and the ecological condition. Relevant changes in coastal ecosystems include mainly man-made modifications, changes in land use and changes in the extent of tidal zones, but also changes in surface structure, elevation and water depth. The Group on Earth Observations – Biodiversity Observation Network (GEO BON) has developed a set of variables, the so called ‘essential biodiversity variables’ (EBV), for the monitoring of biodiversity on a global level. This is later extended with a set of ‘satellite remote sensing EBVs (SRS EBV) variables that can be mapped using satellite data (Pettorelli et al., 2016). Several of these may be relevant for the monitoring of the ecological condition of intertidal zones, such as extent, flooding or atmospheric exposure, or phenology.

1.2 Tides and intertidal zones

Tides

Tides are caused by the effects of the gravitational forces by the moon and the sun, and the rotation of the earth. As the tidal forces depend on the position of the moon and the sun, the tidal range varies both on a daily and a bi-weekly cycle. The maximum tidal range is called spring tide and occurs when the tidal forces of the sun and the moon reinforce each other (at full moon and

new moon); on the other hand, the minimum tidal range is called neap tide and occurs when the sun's tidal force partially cancels the moon's tidal force (Figure 1 and Figure 2). Figure 1 illustrates the different terms that are used for the different tidal water levels.

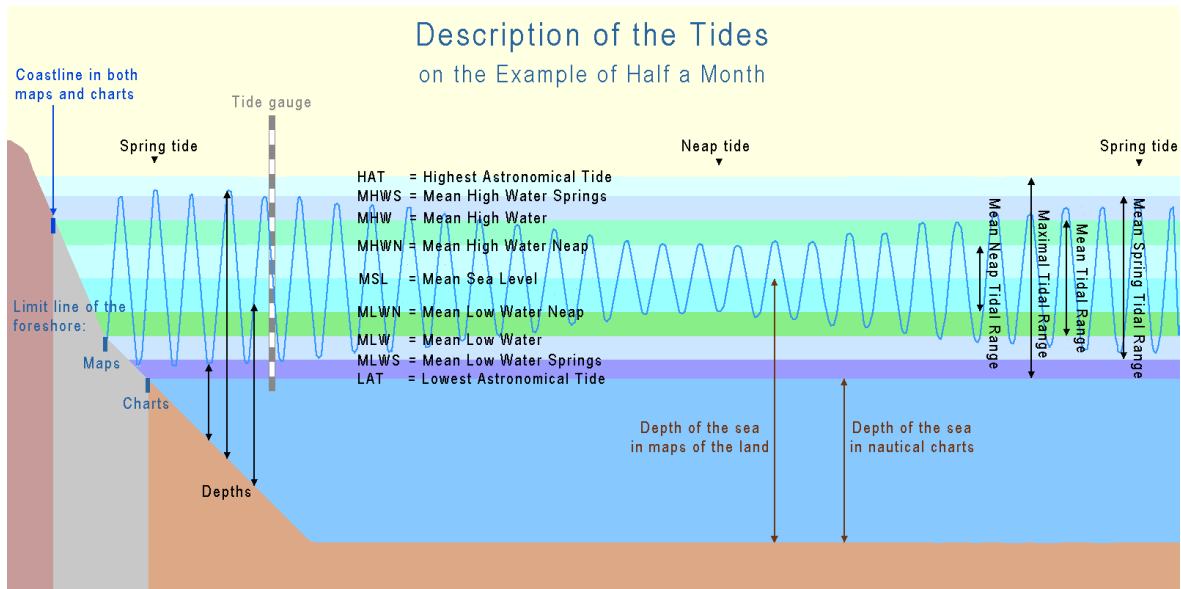


Figure 1. Illustration of tidal terms (Tide Terms by User: Ulamm / Wikimedia Commons / CC-BY-SA-3.0)

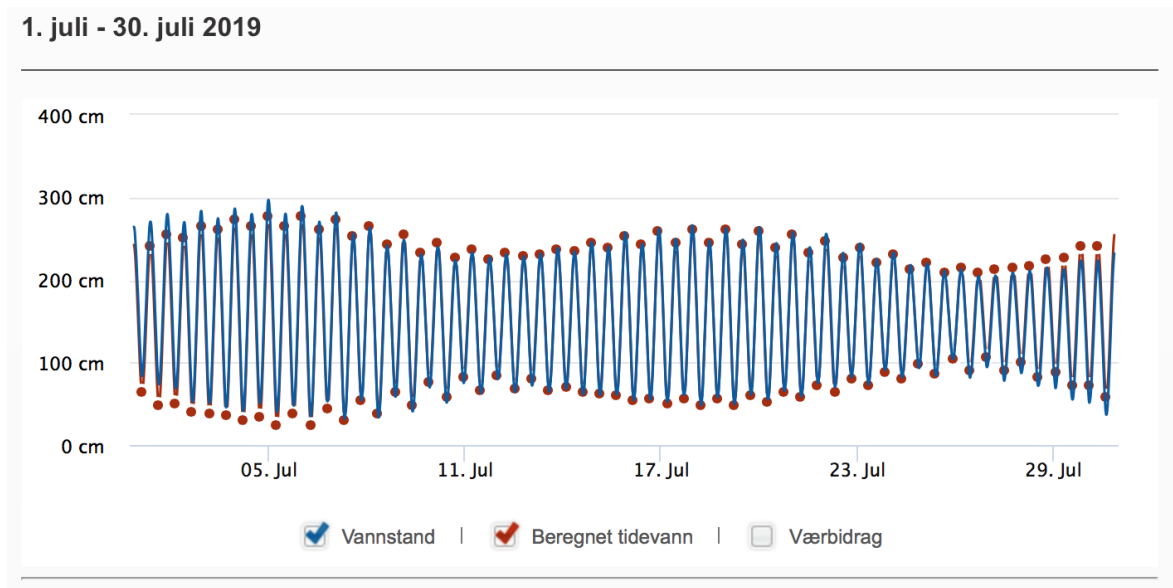


Figure 2. Tidal range variations in Tromsø, July 2019. Tidal data from Se Havnivå (<http://www.kartverket.no>).

In addition to the gravitational forces, the tidal range is also influenced by the weather and the local geography, such as the shape of the coastline and the bathymetry. The tidal ranges inside a fjord or along the outer coast can therefore vary significantly.

The intertidal zones

The intertidal zones are the coastal zones between the high tide and low tide levels; that is, the areas, which are under water at high tides and above water at low tides. Intertidal zones are highly dynamic ecosystems on the transition between marine and terrestrial ecosystems, with major variations in emersion, salinity, temperature, nutrients levels and wave action. The zones are often characterized as having either hard bottom or soft bottom substrates, and include rocky shores, sandy beaches, mudflats, estuaries and saltmarshes.

The intertidal zone is commonly subdivided into 3 zones, although the definition of the boundaries between these vary:

1. *low intertidal zone*: this zone is only above water at the lowest spring tides and is therefore mainly submerged. The low intertidal zone is mainly marine, rich in vegetation (particularly seaweed), and rich in biodiversity.
2. *mid intertidal zone*: this is the area roughly between the average low tide and the average high tide and is therefore regularly exposed and submerged.
3. *high intertidal zone*: this zone is only submerged during high spring tides and is therefore dry most of the time.

There is, however, no single definition or naming convention for the intertidal zone subdivision, and the zone is also often referred to as (eu)littoral zone or foreshore.

1.3 Intertidal zone ecosystems

In Norway, the 'Natur i Norge' (NiN) system (<https://www.artsdatabanken.no/NiN/Systemet>) was developed to describe the variation in nature at 3 different levels: landscape, natural system and environmental living conditions. The natural system is described at three hierarchical levels the main division into 'hovedtypegrupper', 'hovedtyper', and 'grunntyper'. The intertidal ecosystems fall on the transition between the two 'hovedtypegruppene' marine ecosystems and terrestrial ecosystems. The main 'hovedtypene' that occur in the intertidal zone are the marine ecosystems M1 'Eufotisk fast saltvannsbunn', M3 'Fast fjærebeltbunn', and M4 'Eufotisk marin sedimentbunn', and the terrestrial ecosystems T11 'Saltanrikingsmark i fjæresonen', T12 'Strandeng', and T29 'Grus og steindominert strand og strandlinje'. The main differences between these main types are the 1. type of bottom, rock (hard bottom) or unconsolidated sediment (soft bottom); 2. The duration of submersion/exposure: how much of the time is the area exposed to air versus submerged; 3. The presence and type of vegetation (seaweed, salt tolerant grasses).

Ecosystems can be described and distinguished by using a number of relevant environmental variables. Following on from the identification of the main differences between the main ecosystems, the environmental variables that are most relevant for the description of intertidal zone ecosystems are:

1. TV tørrleggingsvarighet: duration of exposure to air, i.e. atmospheric exposure
2. VF vannpåvirkningsintensitet: index describing the influence of water
3. SA marin salinitet: salinity
4. S1 kornstørrelsesklasse: grain size
5. S3 sedimentsortering: indicator for erosion resistance
6. SF saltanriking: salt enrichment
7. IO Innhold av organisk material: organic material content

Not all of these environmental variables will be able to be mapped using remote sensing data, but it is expected that there are a number of variables or indicators that can be mapped which can help distinguish between some of the main ecosystems that occur in the intertidal zone:

1. Tørrleggingsvarighet (atmospheric exposure):
"% of duration of exposure to air" = 100% - "% of duration of submersion"
2. Bottom type: distinction between rocky bottoms and soft sediment bottoms
3. The presence, and possibly type, of vegetation, such as zones rich in seaweed, or areas with salt tolerant vegetation (e.g. coastal meadows ('strandeng'))
4. Man made changes

1.4 Project Objective

The main goal of the project is to develop an efficient method to map and monitor the intertidal zone based on freely available Copernicus satellite data.

The first objective is to develop and demonstrate such a method on Trondheimsfjorden. The sub-goals are to:

- 1) Map the extent of the intertidal zone,
- 2) Identify and classify different types and environmental variables of intertidal zones,
- 3) Detect changes in the intertidal zone,
- 4) Assess the possible use of available aerial photos and processed LiDAR data,
- 5) Propose a concept for large-scale mapping of the intertidal zone for all of Norway on a regular basis.

2. Data

2.1 Demonstration Site - Trondheimsfjorden

The demonstration site to develop the methods is Trondheimsfjorden (Figure 3). The area is in UTM Zone 32N with the following limits:

E 510020 to E 630000,
N 7013000 to N 7112980.



Figure 3. Trondheimsfjorden (©GoogleMaps)

2.2 Satellite data

The use of satellite data is based on the freely available Copernicus program from the European Commission and specifically on the high-resolution radar and optical satellites Sentinel-1 and Sentinel-2.

2.2.1 Sentinel-1

“Sentinel-1 (S1) is a Synthetic Aperture Radar (SAR) mission, providing continuous all-weather, cloud independent, day-and-night imagery at C-band (centre frequency: 5.405 GHz), operating in

four exclusive imaging modes with different spatial resolutions and coverages. Dedicated to Europe's Copernicus Programme, the mission supports operational applications in the priority areas of marine monitoring, land monitoring and emergency management services. The mission is based on a constellation of two identical satellites, Sentinel-1A (S1A) and Sentinel-1B (S1B), launched separately on 3 April 2014 and 25 April 2016. In the interferometric wide-swath mode used here, each S1 can map global landmasses once every 12 days. The two-satellite constellation can deliver a six-day repeat cycle at the equator. The baseline observation scenario is pre-defined. The plan systematically makes use of the same SAR polarization scheme over a given area to guarantee data in the same conditions for routine operational services. More information can be found at <https://sentinel.esa.int/web/sentinel/missions/sentinel-1/observation-scenario> . Sentinel data products are made available systematically and free of charge to all data users including the general public, scientific and commercial users. All data products are distributed in the Sentinel Standard Archive Format for Europe (SAFE) format. More information can be found at <https://sentinel.esa.int/web/sentinel/sentinel-data-access> ." (ESA, online)

The original data format used in this project is Level-1 Ground Range Detected (GRD). "GRD products consist of focused SAR data that has been detected, multi-looked and projected to ground range using the Earth ellipsoid model WGS84. The ellipsoid projection of the GRD products is corrected using the terrain height specified in the product general annotation. The terrain height used varies in azimuth but is constant in range (but can be different for each IW/EW sub-swath).

Ground range coordinates are the slant range coordinates projected onto the ellipsoid of the Earth. Pixel values represent detected amplitude. Phase information is lost. The resulting product has approximately square resolution pixels and square pixel spacing with reduced speckle at a cost of reduced spatial resolution. For the IW and EW GRD products, multi-looked is performed on each burst individually. All bursts in all sub-swaths are then seamlessly merged to form a single, contiguous, ground range, detected image per polarization." (ESA, <https://sentinel.esa.int/web/sentinel/user-guides/sentinel-1-sar/product-types-processing-levels/level-1>)

All acquired Sentinel-1A&B data over the demonstration site Trondheimsfjorden (Figure 4) have been downloaded through the Copernicus Open Access Hub (<https://scihub.copernicus.eu/>) or the Alaska Satellite Facility (<https://vertex.daac.asf.alaska.edu/#>) from 1 January 2017 until 31 December 2018.

Over Norway, the acquisition scenario reflects the maximum acquisition possibilities, continuous acquisition of all paths both ascending and descending. As S1 is polar orbiting, the overlap of the adjacent paths is increasing with latitude and more than 50% around Trondheimsfjorden. Table 1 summarizes the covering paths for one cycle period of 12 days in August 2018, specifying the satellite S1A or S1B, the path number, and the flight direction of the satellite, i.e. 4 ascending (ASC) paths and 3 descending (DES) paths, and the time of overflight. Descending paths pass around 05.45, ascending paths pass around 16.45. All pixels are therefore covered at least 8 times per satellite cycle, i.e. more than 240 times per year. Most of pixels in Trondheimsfjorden are covered at least 26 times per month. Figure 4 also shows the location of the paths and single scenes. Annex 1 shows the full list of acquisitions for 2017 and 2018.

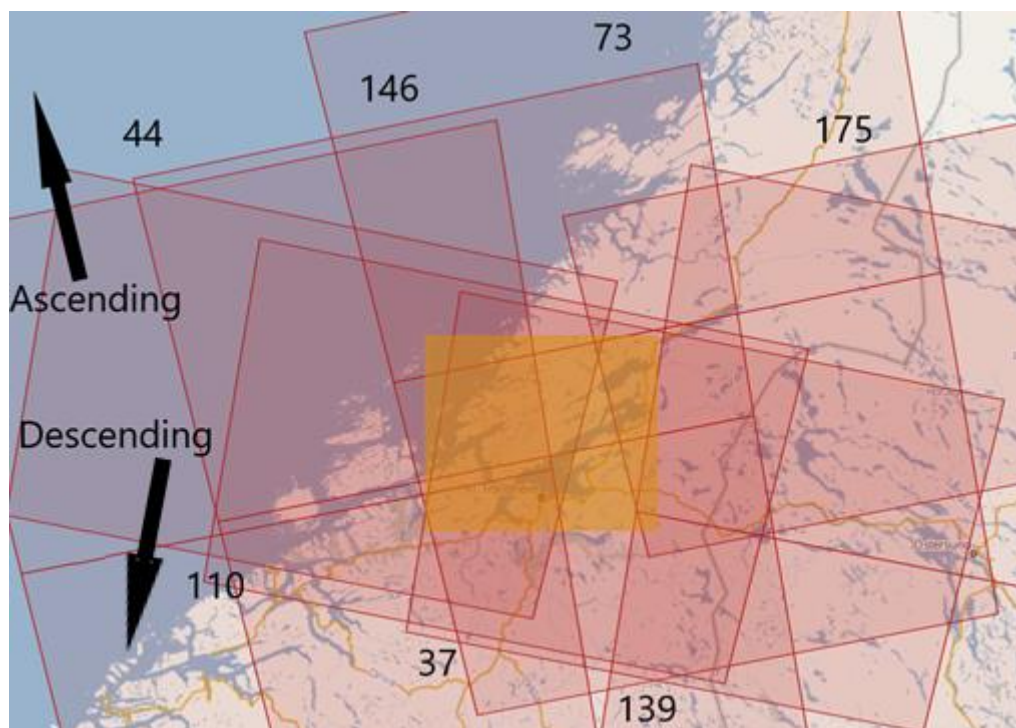


Figure 4. Sentinel-1 paths and coverage of the demonstration area Trondheimsfjorden (yellow rectangle).

Table 1. Sentinel-1 path numbers off a 12-day cycle (starting 01.08.2019) covering Trondheimsfjorden specifying the satellite, path and direction.

Nr	Date	Satellite	Path	Direction
1	01.08.2019 - 05.38	S1B	139	DES
2	01.08.2019 - 16.54	S1B	146	ASC
3	02.08.2019 - 16.46	S1A	073	ASC
4	03.08.2019 - 16.38	S1B	175	ASC
5	05.08.2019 - 05.55	S1A	110	DES
6	06.08.2019 - 05.46	S1B	037	DES
7	06.08.2019 - 17.02	S1B	044	ASC
8	07.08.2019 - 05.38	S1A	139	DES
9	07.08.2019 - 16.54	S1A	146	ASC
10	08.08.2019 - 16.46	S1B	073	ASC
11	09.08.2019 - 16.38	S1A	175	ASC
12	11.08.2019 - 05.55	S1B	110	DES
13	12.08.2019 - 05.46	S1A	037	DES
14	12.08.2019 - 17.02	S1A	044	ASC

2.2.2 Sentinel-2

The Copernicus Sentinel-2 mission acquires optical multispectral satellite imagery in 13 bands in the visible, near infrared and short wave infrared part of the spectrum (Table 2) at a high spatial resolution (10 - 60 m) and with a swath width of 290 km (<https://sentinel.esa.int/web/sentinel/missions/sentinel-2>). The mission consists of 2 polar-orbiting satellites, Sentinel-2A and Sentinel-2B, which provide a revisit time of 5 days at the equator and 2-3 days in Norway. The spectral bands are chosen such that they provide spatial information on land cover/land use, vegetation properties, cloud/snow separation, which can be used for applications in environmental monitoring (e.g. land cover change, effects of climate change), land management (e.g. crop monitoring for agriculture, forestry), estimation of vegetation biophysical parameters (e.g. leaf chlorophyll content (Ch), leaf area index (LAI)), mapping of coastal zones, monitoring of inland waters, snow cover, or risk management (e.g. flood mapping). The Sentinel-2 satellites provide continuity for the multispectral imagery provided by the Landsat TM and SPOT satellites, and, in addition, include three new narrow spectral bands in the red edge region (680 – 730 nm; Table 2), which significantly improve the estimates of biophysical parameters Ch and LAI (Delegido et al., 2011). The data is freely available from the Copernicus Open Access Hub or the national Norwegian hub (<https://colhub.met.no/#/home>). Sentinel-2 data is available for download in 2 main formats, level 1-C and level 2-A. The level 1-C product includes radiometric and geometric corrections and represents the top-of-atmosphere (TOA) reflectance; the level 2-A product includes an atmospheric correction applied to the level 1-C product and represents a bottom-of-atmosphere (BOA) reflectance.

Band number	Description	Central wavelength (nm)	Band width (nm)	Spatial resolution (m)
1	Coastal aerosol	443	21	60
2	Blue	493	66	10
3	Green	560	36	10
4	Red	665	31	10
5	Vegetation red edge	704	15	20
6	Vegetation red edge	740	15	20
7	Vegetation red edge	783	20	20
8	NIR	833	106	10
8a	Vegetation red edge	865	21	20
9	Water vapor	945	20	60
10	SWIR – Cirrus	1374	31	60
11	SWIR1	1610	92	20
12	SWIR2	2190	180	20

Table 2. Band specifications Sentinel-2 (<https://sentinel.esa.int/web/sentinel/user-guides/sentinel-2-msi/resolutions/radiometric>).

In this study, all Sentinel-2A and 2B images from 2018 (between 1st March and 30th October 2018) over Trondheimsfjorden, with a cloud cover of less than 20% were used within, as level 2-A orthorectified atmospherically corrected surface reflectance products, as available within google earth engine.

2.3 Aerial and ground reference data

2.3.1 Aerial photos from Norgebilder.no

Norgebilder.no is a cooperation between Statens vegvesen, Norsk institutt for Bioøkonomi (NIBIO) og Statens kartverk, providing an overview of aerial photos over Norway that cooperating partners in the “Norge digital” program acquired as ortho-photo mosaics. Norge digital is a cooperation between the public agencies that have responsibilities for producing or using geodata. Publishing in Norgebilder.no is also open to other data providers.

This project was given access to the database of the aerial mosaics. The aerial ortho-mosaics have each their individual meta data set and specifications and it is therefore not a homogenous data base with equal quality, resolution etc, nor predefined acquisition plans. The meta data provided for each mosaic has the following information:

Name and acquisitions year: f.e. Nord Trøndelag 2017

Fotodate: f.e. 2017-06-30

Publising date: f.e. 2017-12-15

Prosjektstart: f.e. 2017

Data owner: f.e. Omløpsfoto

Type: f.e. Ortofoto 50

Resolution: f.e. 0.25 (m)

Mappingnumber f.e. TT-14313

Image category: f.e. Color

Color coding: f.e. 24 bit/px

Acquisition method/sensor: f.e. Digital sensor

Picture format: f.e. TIFF

Orientation method: f.e. GNSS/INS med AAT

Coordinate system: f.e. UTM32 EUREF89

Flight: f.e. TerraTec AS

Producer: f.e. TerraTec AS

A product specification report.

The general resolution of the aerial data is in the range of 10cm to 1m. And the main type are aerial photos in visible wavelength. Some infra-red acquisitions are also available. Unfortunately, there is no specific time information or acquisition time period available, neither with the meta data, nor in the product specification reports, so it is not possible to compare this data set with the tidal charts. It is just by comparison between different data sets over the same region that one can roughly estimate high, middle or low tide.

Because of its high resolution, this data base is still a good source of ground truth data with regard to some tidal zone types and the presence of vegetation or algae. However, the waterline is generally difficult to see or extract exactly. This data set is so inhomogeneous and misses

necessary time information to be used operationally on large areas. It is, however, a good source to detect and identify changes, and to help interpret the different types of tidal zones.

2.3.2 Vector data from “Naturbase”

The GIS database Naturbase from the Norwegian Environment Agency combines GIS based environmental data from a range of different sources in Norway, including data from the Norwegian Environment Agency, NIBIO, NINA, Norwegian Polar Institute, Artsdatabanken, and Institute of Marine Research. Data available in this database that is relevant for tidal zone mapping includes data on protected sites, and data on selected ecosystems. This includes GIS data on marine ecosystems, such as mudflats (bløtbunn), large kelp forests, coastal meadows and wetlands and occurrences of shell sand. This data is potentially useful as ground truth data to either train or validate the results from the satellite image analysis. However, a challenge with these datasets is that the vector outlines are generally manually digitized, presumably based on visual interpretation of aerial photographs (according to the measurement method description in the metadata: ‘digitized on screen from orthophotos’). The vector outlines can be rather coarse and include other adjacent ecosystems, which can make it difficult to compare directly with the results of satellite image analysis. They are also not always complete, but often only include well known examples or important protected sites. On the other hand, they are useful as examples of where certain coastal and marine ecosystems are known to occur, which helps with the visual interpretation of aerial photographs to create training data. The most useful and complete vector dataset for this project is the mudflats dataset, which will be used as comparison in some of the figures shown in chapters 3 and 4.

2.3.3 In-situ data

Field data was collected in the Grindøysundet nature reserve on Kvaløya, close to Tromsø, on 19 July 2019. This area is part of the Ramsar site Balsfjord wetland system, with extensive mud- and sandflats with coastal meadows. Low tide on the day of the visit was at 09:59, with a predicted water level of 49 cm (Se Havnivå: <http://www.kartverket.no>); the site was visited around low tide, from ca 09:30 to 11:20, with an estimated tidal water level between 49 and 68 cm, which is around the mean low water spring tide level of 51 cm in Tromsø (Kartverket, 2019). During the field visit, ground photography with GPS coordinates were taken to identify different ecosystems. A GPS track was recorded along the water line starting ca 30 min before the lowest tide until about 1.3 hour after the lowest tide. The track is shown under the validation section and is used for the accuracy assessment of the intertidal zone extent.

3. Methods

3.1 Pre-processing

3.1.1 Sentinel-1 CSAR

Norut's (now NORCE's) GSAR/GDAR SAR processing system is used in this project as it allows operational processing of big data. The system had been set-up for Troms and adapted to Trondheimsfjorden and the process has been streamlined into the three following steps:

- 1) Geocoding and radiometric calibration
- 2) Radiometric slope correction according to Ulander (1996).
- 3) Yearly and monthly statistical analysis of data stack and mosaics production

All scenes have been pre-processed in UTM zone 32N in 20m resolution.

The S1 GRD data over Trondheimsfjorden was pre-processed with Norut's (NORCE's) geocoding software (Larsen et al., 2005) using the 10m Norwegian digital elevation model. Header information in the S1 *.SAFE folder include the necessary parameters for radiometric calibration and the exact satellite orbit information for georeferencing and terrain correction with the DEM. GRD files are therefore directly converted into georeferenced, radiometrically corrected gamma-naught γ^0 radar backscatter images in dB for both polarization, co-polarization VV and cross-polarization VH, $\gamma^0(VV)$ and $\gamma^0(VH)$, respectively.

Single scenes of the same orbit are directly processed together into one continuous image.

Once the GRD data are processed into georeferenced and radiometric corrected images an additional radiometric slope correction according to Ulander (1996) is applied. This is less relevant in this project as the topography in the intertidal zone is not resolved in the DEM.

Instead of using Norut's internal software that is set up for large scale operational monitoring, the pre-processing step can also be done with ESA's free openly available Sentinel 1 Toolbox from the Sentinel Application Platform (SNAP). As far as we understand should the Norwegian Ground segment also provide such pre-processed data, but the usage of this data has not been evaluated in this project.

3.1.2 Sentinel-2

The S2 surface reflectance images in google earth engine are already radiometrically and atmospherically corrected. The QA60 band, which is created during the level-2A processing, has been used to mask clouds and cirrus. The dataset is filtered to exclude scenes with more than 20% cloud cover prior to further processing.

3.2 Intertidal-zone mapping

The intertidal zone can be observed with both optical and radar satellite imagery. Since the intertidal zones are highly dynamic areas with twice daily submersion and exposure, it is necessary to use satellite time series to catch the range of tidal stages. Optical satellite data has the additional challenge with frequent cloud cover in Norway, which reduces the number of cloud free images available and requires additional preprocessing to mask pixels that are affected by cloud cover. In this section we describe in detail the methods used to analyze optical and radar satellite imagery to identify intertidal zones and distinguish different ecosystems.

3.2.1 Intertidal-zone area mapping with Sentinel-1 CSAR

The approach to map the intertidal zone with Sentinel-1 is straight forward. The radar backscatter signature from water and land are quite distinguishable and can be generally separated by thresholding. As the tidal phase is half a moon-day, i.e. 12h 25.2 min and Sentinel-1 passes are approximately at the same times of the day, either around 5.45 for descending paths or 16.45 for ascending paths, the phase difference and a long time series insure that acquisitions are taken both at lowest and highest storm tides. Every 12-day satellite cycle corresponds to a tidal phase shift of 4.8 min. Inside a 12-day satellite cycle, each pixel in Trondheimsfjorden is observed at least 8 times. Inside the intertidal zone area, the signatures will therefore vary strongly between low backscatter when covered by water and high backscatter when exposed to the atmosphere. The highest and lowest waterline can therefore be extracted by thresholding the image representing the highest and lowest percentile of a backscatter time series. Figure 5 shows the low and high percentile images from the 2017-2018 data series.

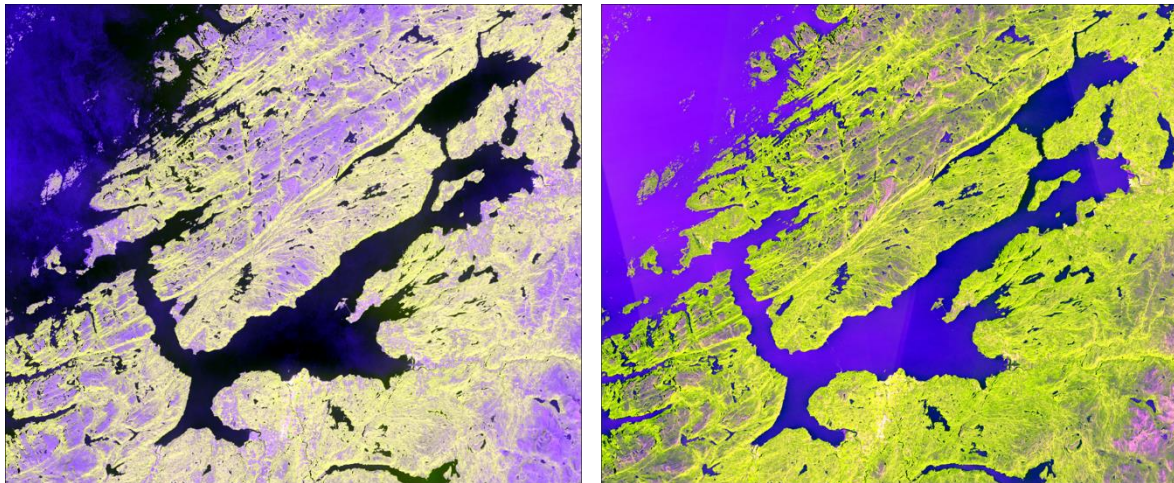


Figure 5. Low percentile (minimum, left) and high percentile (maximum, right) backscatter mosaics over Trondheimsfjorden. RGB=[VV,VH,NDI].

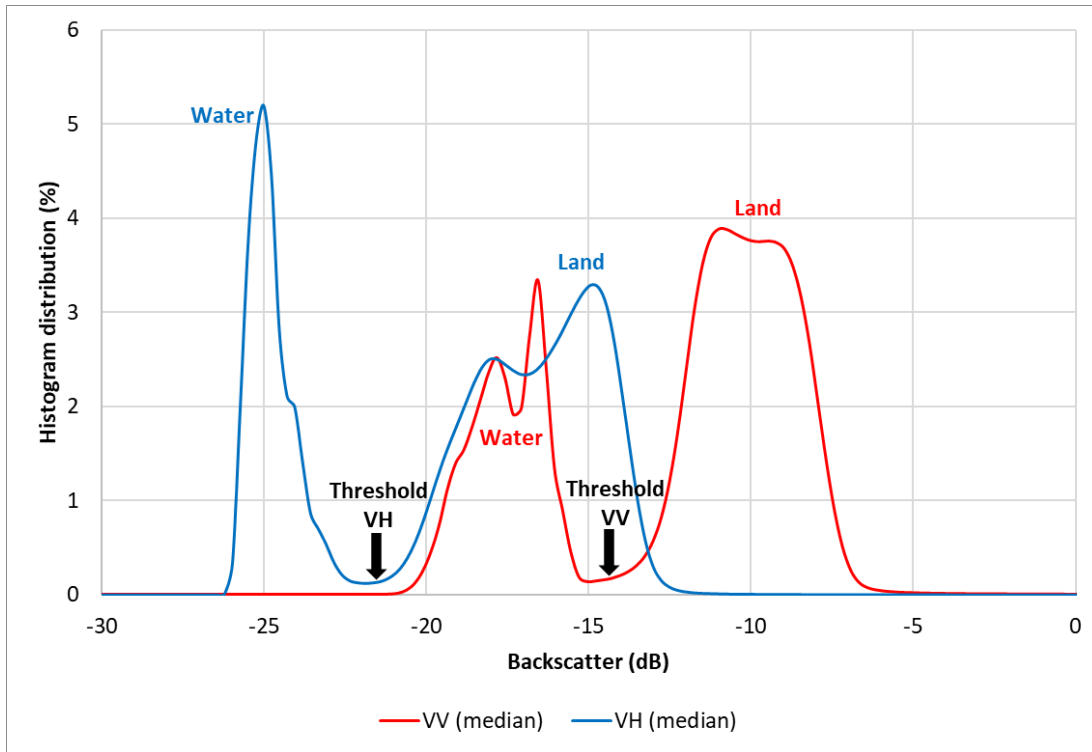


Figure 6. Median value (50 percentile value) VV and VH backscatter histogram over the Trondheimsfjorden area from Sentinel-1 2018 data. The left mode represents backscatter over water and the right mode, backscatter over land for both polarizations, VV and VH.

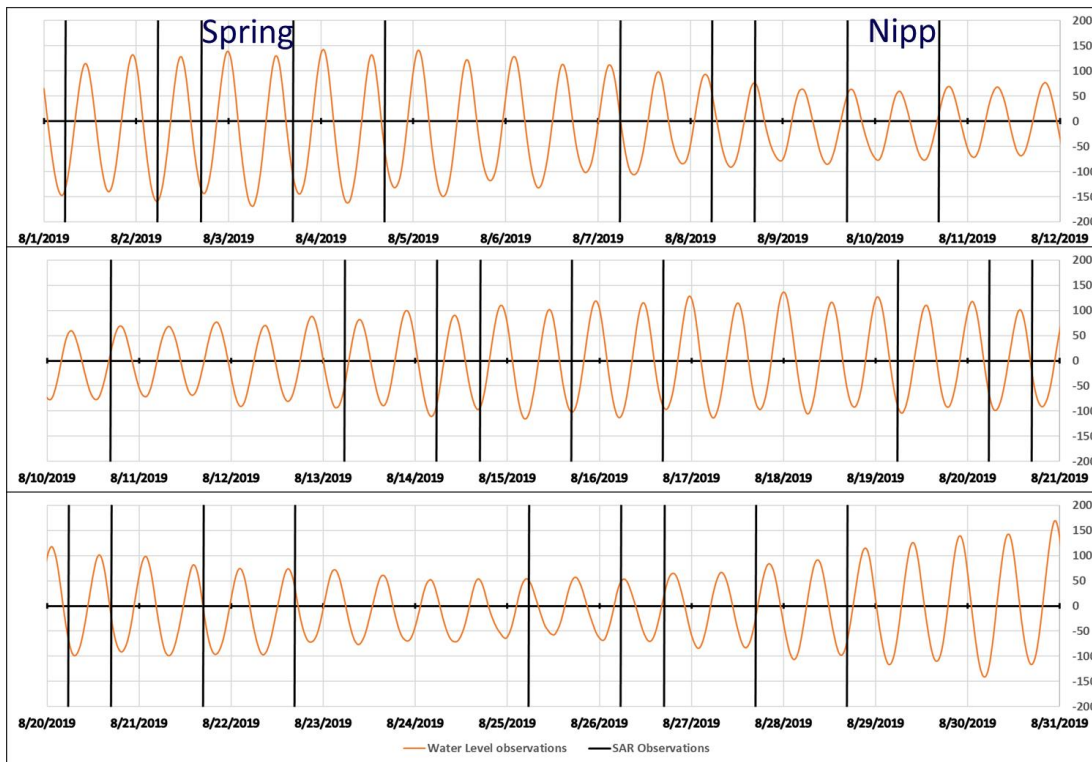


Figure 7. Tidal chart for Trondheim for August 2019 with the Sentinel-1 overpasses indicated with black bars.

The tidal chart (Figure 7) of Trondheim for August 2019 and the S1 acquisition marked as black bars illustrate the approach. The method can therefore be separated in 3 steps:

- 1) Preprocessing (geolocating , radiometric and topographic correcting) all Sentinel-1 data from a long time series
- 2) Statistical analysis of the backscatter time-series for each pixel, providing backscatter images that represent high and low percentiles of backscatter.
- 3) Extracting the high and low water lines by thresholding low and high percentiles, for example 2 and 98 percentile, respectively.

The intertidal zone is then the area between the high and low waterlines extracted from the lowest and highest percentile backscatter, respectively.

As a first approach over Trondheimsfjorden, the percentile extraction was not included in our software, so first results from Trondheimsfjorden have been based on the median value from monthly maximum and minimum backscatter values over the years 2017-2018. During this project the percentile extraction tool has been improved and included in the software and we use the 2% and 98% percentiles extracted from a two-year time series in order to limit the speckle noise. This has been done for the accuracy assessment.

Comparison with field data and high-resolution aerial data showed that water-land thresholds at low tides (high percentile, 98 percentile image) are in the range of [-8dB, -7dB] for the VV and [-21dB, -16dB] for the VH backscatter. For high tides (low percentiles, i.e. 2 percentile image), the VV and VH thresholds are in the range of [-25dB, -19dB].

The precise definition of the threshold has been derived from the histograms, comparison with high resolution data and considering noise for the highest and lowest percentile.

The water land threshold for the 2 percentile backscatter values have been determined to be -16.5 dB and -24.5 dB for VV and VH. This corresponded also quite well to the land mask extracted from the 10m, thresholding at 10cm and represents in fact an update of the land mask for the years 2017/2018. We thereby define the water line of the highest tide and the reference land mask by:

$$\text{Land mask} = (\text{DEM} > 0.5\text{m}) \text{ OR } ((\gamma_{\text{VV}}(2 \text{ perc.}) > -16.5\text{dB}) \text{ AND } (\gamma_{\text{VH}}(2 \text{ perc.}) > -24.5\text{dB}))$$

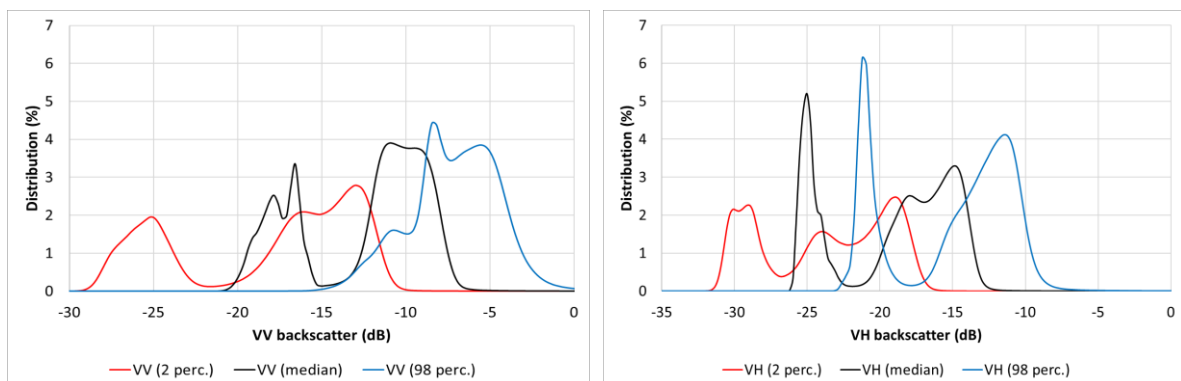


Figure 8. 2 percentile, median value (50 percentile) and 98 percentile Sentinel-1 VV and VH image histograms over the Trondheimsfjorden area from 2018 data.

The water land threshold for the 98 percentile backscatter values have been determined to be -7.30 dB and -17.87 dB for VV and VH. At such high percentiles, strong wind events over the ocean during the observation can induce noise particularly at low radar incidence angles at near range. In Sentinel-1 data we therefore cut off the acquisitions taken at incidence angles lower than 32.2 degree.

The method is applied on 10m resolution interpolated images from the original 20m-resolution pre-processed data.

The legend of the final results is shown in Figure 9.

Intertidal Zone Area		
Class	Color Code	Pixel Values
Land		8
Intertidal Zone Area		1
Water		0

Figure 9. Legend of the Intertidal Zone Area products

3.2.2 Intertidal zone area and type mapping with Sentinel-2

The methodology used for the analysis of Sentinel-2 data for the purpose of mapping tidal zones uses statistical parameters calculated from time series of several vegetation and water indices and is inspired by the methodology presented by Murray et al. (2019). The reason behind using time series is that tidal zones are very dynamic areas, which are submerged some or most of the time. This makes it difficult to image the areas at low tides. By using cloud-free time series, the area is imaged at different tidal stages and the variation in index values with time is expected to help distinguish between permanent water, permanent land and tidal zones. The processing workflow has been implemented in java script within Google Earth Engine (GEE; Gorelick et al., 2017), which provides cloud-based access to satellite imagery and enables the analysis of large datasets in the cloud.

The diagram in Figure 10 summarizes the workflow used in this project and the different steps will be described in more detail below. All steps, apart from the visual comparison with aerial photographs and class reduction (in step 4) were carried out in GEE. The visual comparison and class reduction were carried out in QGIS in combination with python.

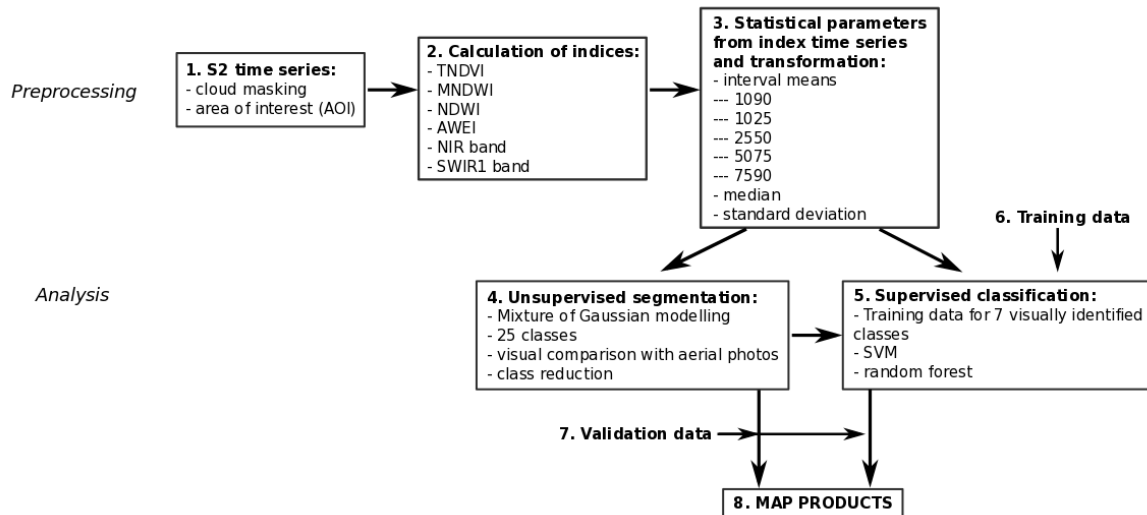


Figure 10. Processing workflow used for Sentinel-2.

- Optical satellite imagery is dependent on cloud free conditions and cloud covered areas will therefore need to be masked. Level 2-A S2 imagery has been atmospherically corrected and includes information on cloud cover in the QA60 band. The information in this band has been used to mask cloud covered pixels in each image used in the analysis. All available images in the period between 1st March 2018 and 30th October 2018, covering the study area Trondheimsfjorden, and with less than 20% total cloud cover, were used. Figure 11 shows that, after cloud masking, each pixel was covered by between 15 and 73 images. In addition to cloud masking, all areas outside the tidal zone region were masked by creating an area of interest (AOI); the AOI is here defined as the zone within 2 km of the coastline, and at elevations of less than 2 m (based on the 10 m DTM from <http://www.geonorge.no>). The mask was created in QGIS, using a coastline vector downloaded from <http://www.geonorge.no> in combination with the 10 m DTM.
- Two vegetation indices and three water indices were calculated for each image: the transformed normalized difference vegetation index (TNDVI), the normalized difference vegetation index (NDVI), the modified normalized difference water index (MNDWI), the normalized difference water index (NDWI), and the automated water extraction index (AWEI). These indices provide information about the presence and greenness of vegetation and the presence of surface water. In addition to the indices, the NIR band (band 8) and SWIR1 band (b11) are also included and help distinguish land and water and provide information on vegetation biomass. The vegetation and water indices are calculated using the following equations and band combinations; Table 2 described the different band numbers that are used.

$$(1): TNDVI = \sqrt{\frac{(b8-b4)}{(b8+b4)}} + 0.5$$

$$(2): NDVI = \frac{(b8-b4)}{(b8+b4)}$$

$$(3): MNDWI = \frac{(b3-b11)}{(b3+b11)}$$

$$(4): NDWI = \frac{(b3-b8)}{(b3+b8)}$$

$$(5): AWEI = 4 \times (b3 - b11) - (0.25 \times b8 + 2.75 \times b12)$$

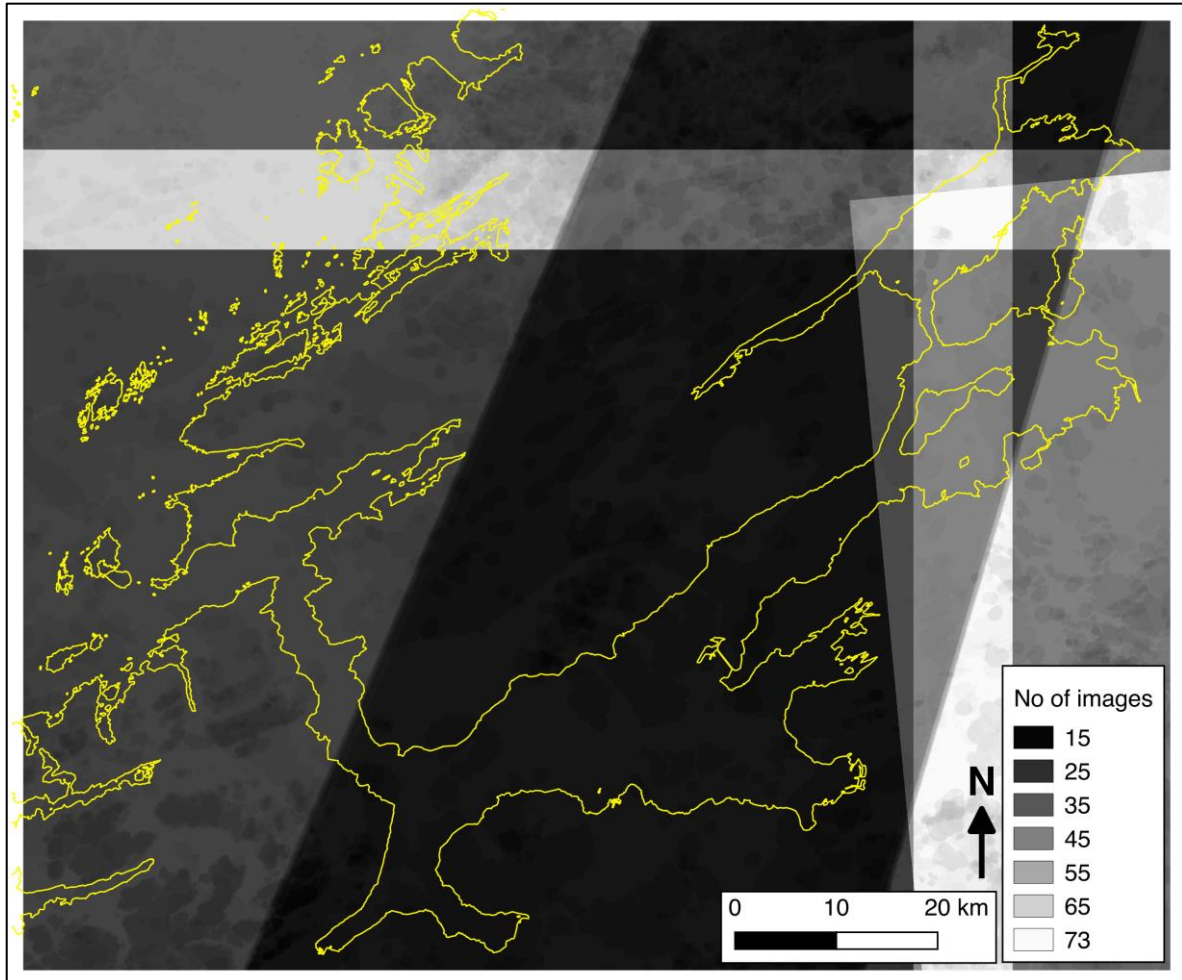


Figure 11. Number of images used in the analysis after cloud masking.

3. To reduce the amount of data and get different measures of the temporal variation of the indices and NIR band, a number of statistical parameters were calculated from the time series: interval means, median and standard deviation (sd). An interval mean is the mean of the data within a percentile range; e.g. the interval mean 1090 is the mean of the data in the percentile range 10 to 90. The interval means contain information about the shape of the distribution. Four of the parameters did not show a Gaussian distribution (NIR mean, NIR median, NIR sd, and AWEI sd) and were first transformed using a log transform. All parameters were subsequently normalized to distributions with a mean of 0 and sd of 1.
4. Both supervised (step 5) and unsupervised clustering was performed on the statistical images. Unsupervised clustering was done using a multivariate Gaussian mixture model (GMM), which assumes that the dataset consists of a number of Gaussian distributions, each defined by a mean and variance. The GMM models the dataset to identify the

number of distinguishable Gaussian distributions and then calculates the probability that a pixel belongs to one of these distributions. The advantage of the GMM over the commonly used K-means clustering method is that it is based on probabilities rather than distances to cluster centers, and that it takes into account that the different distributions have different shapes (different means and variances). The result of the clustering was then visually investigated against aerial photos to identify what each of the distinguished clusters (classes) represented; several of the clusters were combined into a single class and the original 25 classes were reduced to 7.

5. For the supervised classification, a database with training polygons was created based on visual interpretation of aerial photographs (Norge-i-Bilder) (step 6). The training polygons were used to train a random forest classifier, which was subsequently applied to the whole image. A simple smoothing filter was applied to reduce some of the speckle.
6. Training data is based on the visual interpretation of aerial photos. All available aerial photos of key areas with extensive intertidal zones (e.g. Grandefjære, Tautra, Storfosna) were checked and the photos taken at the lowest tidal levels were downloaded. A number of classes were visually identified, and examples were digitized on screen to create a database with training data (Figure 12). A total of 85 polygons were created identifying 7 classes: permanent water, land, mudflat, sandy/gravel beach, rocky shoreline, seaweed, and shallow water.

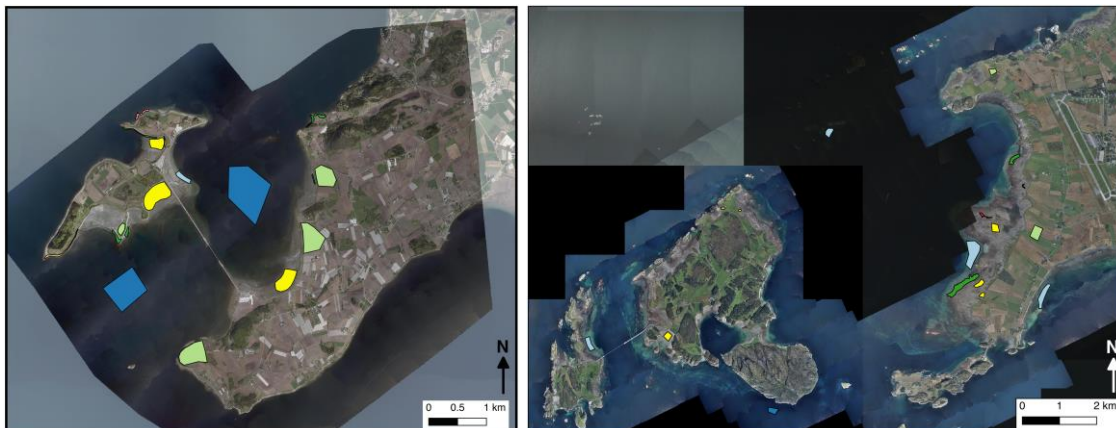


Figure 12. Example of training polygons in areas around Tautra (left) and Grandefjære (right).

7. Initial validation is done visually against the aerial photos. In addition, a validation set of stratified random sample points was generated: stratified based on the classes in a classified product, with 50 random samples per class. The points will be classified visually and compared to the classified image to estimate the accuracy.
8. The generated products include a map of the occurrence and extent of tidal zones, and a map showing more detail in the tidal zones, identifying intertidal pools, bands of seaweed, rocky outcrops, mudflats and shallow water.

3.2.3 Intertidal zone type mapping with Sentinel-1

Training polygons that have been collected when developing methods for inter-tidal zone type mapping with Sentinel-2 have been also used for testing a maximum likely hood (MLH) classifier and a neural networks (NN) classifier from the ENVI software applied on the Sentinel-1 percentile images. 4 different runs were performed:

- MLH classification using the whole set of percentiles and the mean SAR images of both polarization VV and VH,
- MLH classification using only the 98 percentile images of VV and VH.
- NN classification using the whole set of percentiles and the mean SAR images of both polarization VV and VH,
- NN classification using only the 98 percentile images of VV and VH.

The legend of the intertidal zone type maps is shown in Figure 13








Intertidal Zone Type		
Class	Color Code	Pixel Values
Land		8
Mudflat		5
Rock		4
Sand		3
Seaweed		2
shallow water		1
water		0

Figure 13. Legend of Intertidal Zone Type maps.

3.2.4 Use of aerial data

Aerial data from Norge-i-Bilder has been visually investigated, and it was concluded that the aerial data is not suitable for operational and large-scale monitoring of intertidal zones. There are several reasons for this:

- 1) The aerial data, as it is available on norgebilder.no, only comes with a time stamp of the date, but not the exact time of the acquisition. That is also quite logic in the way that the aerial data is available as mosaics of aerial photography and not as single photographs. Since there are no time stamps, it is impossible to combine this data with modeled or observed tidal heights.
- 2) To map intertidal zones, it would be necessary to have acquisitions at both maximum low and maximum high tide, which has obviously not been considered in the strategy under the acquisition of the aerial data.
- 3) Tidal maximums can vary over relatively short distances because of the fjord systems along the Norwegian coast. So even if we would know the exact time at some position, it would be difficult to extract this over the whole region.
- 4) Aerial photos over Norway are of different quality and resolution, as they have been taken under different light conditions and with different cameras, which makes a consistent method difficult for nation-wide intertidal zone area mapping.

- 5) The access and quantity of the aerial data over all of Norway for processing would be very challenging for processing on a large scale. It would be either necessary to download the whole data or bring the method to the data in the cloud.
- 6) Investigating several aerial mosaics has also shown that it is nearly impossible to distinguish the water line in the optical data, especially under calm water condition. That is even the case when using aerial photos for validation of the results presented in this report.

Nevertheless, the high resolution of aerial data gives us important information to help distinguish different types of intertidal zone. It is therefore used to establish training data for classification of the intertidal zone and validation data for the results. Exact interpretation however is still challenging and the quality of any training and validation data set will still be dependent of the analyst's experience.

3.3 Mapping of atmospheric exposure ("Tørrleggingsvarighet") with SAR

Similar to the extraction of the water line at lowest and highest tide with thresholding high and low percentile images based on a statistical analysis, a water line extracted from thresholding a percentile image P of the backscatter time series corresponds to a certain atmospheric exposure time of $100\% - f(\text{percentile } P)$.

As a first approach we have extracted the percentile images of 2%, 5%, 25%, 50%, 75%, 95% and 98 % percentile from the 2017-2018 Sentinel-1 time series and extracted the minimum between the land and water modes (see Figure 6) from each of these backscatter distributions. Figure 14 and Figure 15 show the backscatter distribution of VV and VH backscatter at these percentile levels.

This has been done for each year 2017 and 2018 separately in order to get a measure of robustness of this approach. Table 3 summarizes the land water threshold for each of the percentile images. The threshold of 2017 and 2018 are stable in a range of $\pm 0.25\text{dB}$. As a minimum threshold however, we use the same threshold as for the establishment of the highest water line in 3.1., i.e. -16.5 dB and -24.5 dB for VV and VH, respectively. The final land-water thresholds $\gamma_{VV}(\text{perc.})$ and $\gamma_{VH}(\text{perc.})$ are marked in bold in Table 3.

Table 3. Land-water threshold values for VV and VH backscatter for the percentile images of 2%, 5%, 25%, 50%, 75%, 95% and 98 % percentile for each year 2017 and 2018.

VV	2%	5%	25%	50%	75%	95%	98%
2017	-21.66	-20.69	-17.50	-14.81	-12.05	-8.73	-7.30
2018	-21.54	-20.29	-17.79	-15.05	-12.15	-8.89	-7.39
$\gamma_{VV}(\text{perc.})$	-16.50	-16.50	-16.50	-14.81	-12.05	-8.73	-7.30
VH	2%	5%	25%	50%	75%	95%	98%
2017	-26.19	-25.38	-23.44	-22.04	-20.54	-18.97	-18.00
2018	-26.69	-25.46	-23.35	-21.89	-20.46	-18.88	-17.87
$\gamma_{VH}(\text{perc.})$	-24.50	-24.50	-23.35	-21.89	-20.46	-18.88	-17.87

Figure 16 shows the land-water threshold as a function of percentile level. It seems that between 5 and 95% the relationship could be modeled linearly.

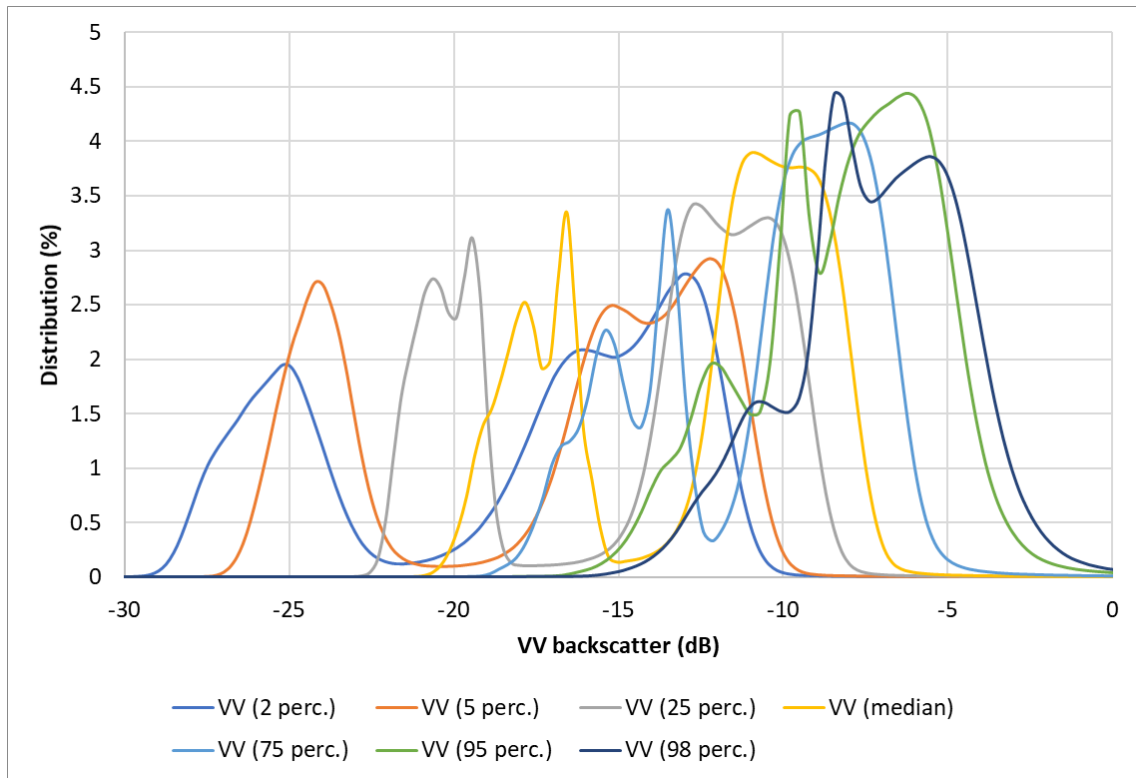


Figure 14. VV Backscatter distribution of percentile images at 2%, 5%, 25%, 50%, 75%, 95% and 98 % percentile.

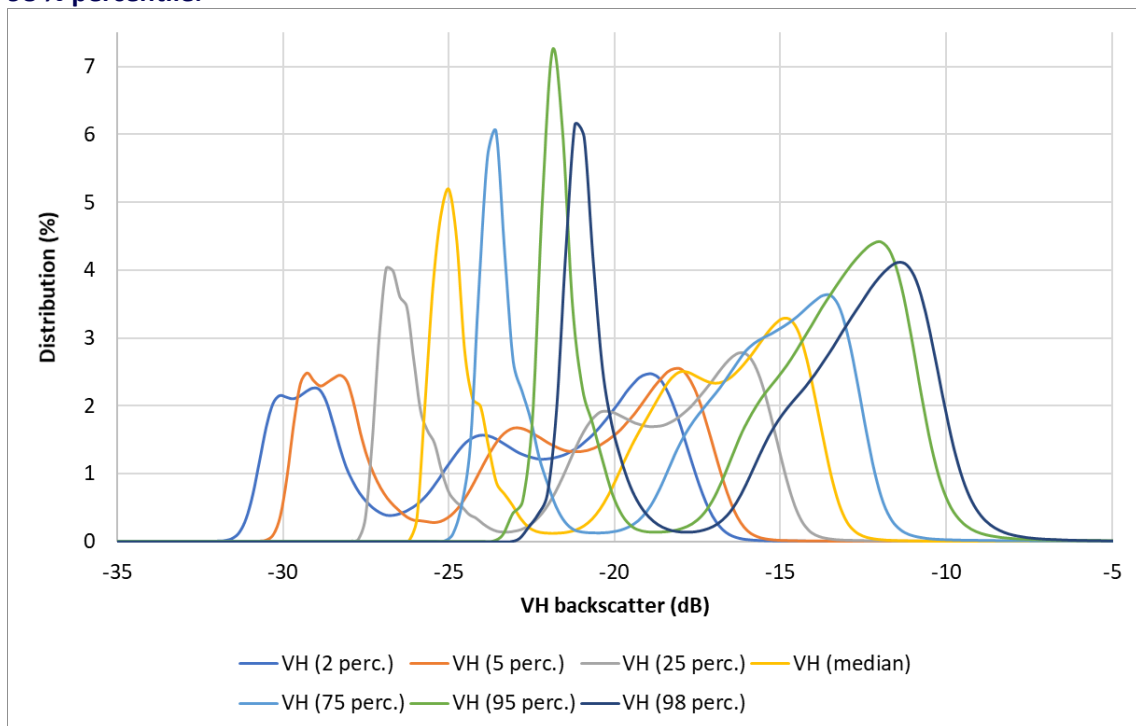


Figure 15. VH Backscatter distribution of percentile images at 2%, 5%, 25%, 50%, 75%, 95% and 98 % percentile.

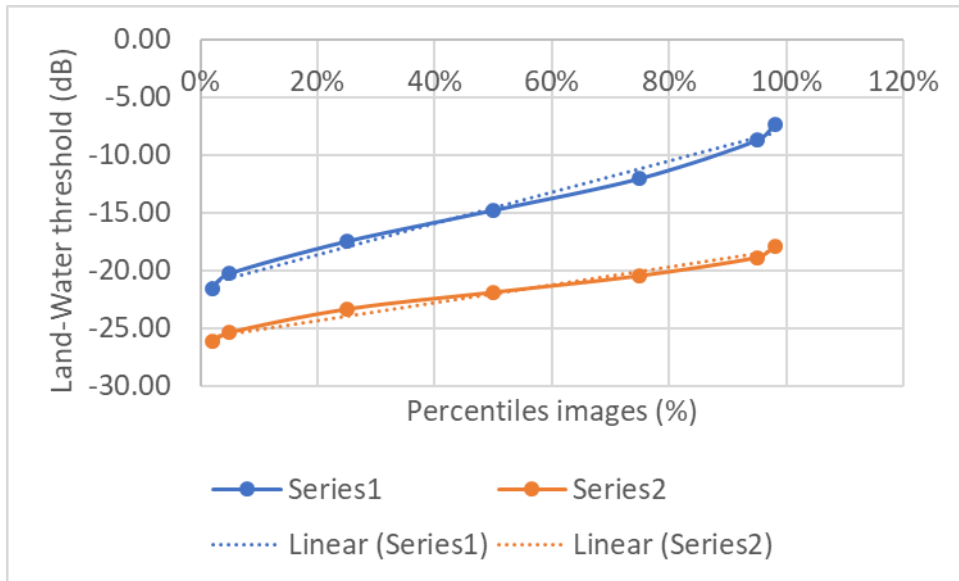


Figure 16. Land water threshold vs percentile image for VV and VH polarizations.

Therefore, for a certain percentile P, the corresponded land-water thresholds $\gamma_{VV}(P)$ and $\gamma_{VH}(P)$ each define the threshold of the atmospheric exposure $AtmEX(100\%-P)$. by

$$AtmExp(i,j) > 100\%-P \quad \text{if} \quad \gamma_{VV}(i,j) > \gamma_{VV}(P) \text{ OR } \gamma_{VH}(i,j) > \gamma_{VH}(P).$$

The method has been applied on the 10m-resolution interpolated percentile images and the legend of the results is shown in Figure 17.

ITZ - Atmospheric Exposure (Tørreleggingsvarighet)		
Class	Color Code	Pixel Values
Land (DEM >50cm)	Black	8
Land (mask from S1)	Brown	7
95-100%	Red	6
75-95%	Orange	5
50-75%	Yellow	4
25-50%	Light Green	3
5-25%	Bright Green	2
1-5%	Cyan	1
Water	Blue	0

Figure 17. Legend of Intertidal Zone Atmospheric Exposure maps.

3.4 Mapping of intertidal zone changes

Most of the intertidal zone definition, specifically the water level lines are all defined as “mean” values, which necessitates a certain integration period for defining natural changes. Rapid changes from anthropogenic activities and disasters should be detectable using shorter integration times, like on a monthly basis directly by comparing single SAR scenes; however likely to show noise at high resolution because of SAR speckle noise.

Yearly changes can be directly detected through comparison of specific percentiles over long time period. The highest percentile should detect most changes. Changes above the highest water line, like for example man made above-water constructions should also be detectable at lower percentiles if they have occurred during the whole integrated time period. Otherwise the level of percentile that detects the changes is directly related to the period since the change has occurred. This means that different percentiles could be used to approximately date the change.

A general threshold to detect changes used in SAR remote sensing is +3dB or -3dB difference between images of different periods for both VV and VH polarization. Lower thresholds of differences might detect noise and natural backscatter variations. Results from subtracting high percentile images of 2017 from 2018 show some first example and man-made construction and changes are clearly detectable. Natural changes in the intertidal zone might occur on longer time scales and needs therefore a longer acquisition and processing of Sentinel-1 data.

Annual changes can also be investigated through direct comparison of classified products derived from (un)supervised classification of S2 annual time series.

4. Results

4.1 Intertidal Zone Area Mapping

4.1.1 Intertidal Zone Area Mapping with Sentinel-1

The final results of the intertidal zone are based on the time series for all data available in the 2017-2018 period using the method described in section 3.2.1. The final results of the intertidal zone area product is presented in Figure 18, the intertidal zone area superimposed on the Sentinel-1 mosaic in Figure 19 with zoom-ins in Figure 20 -22.

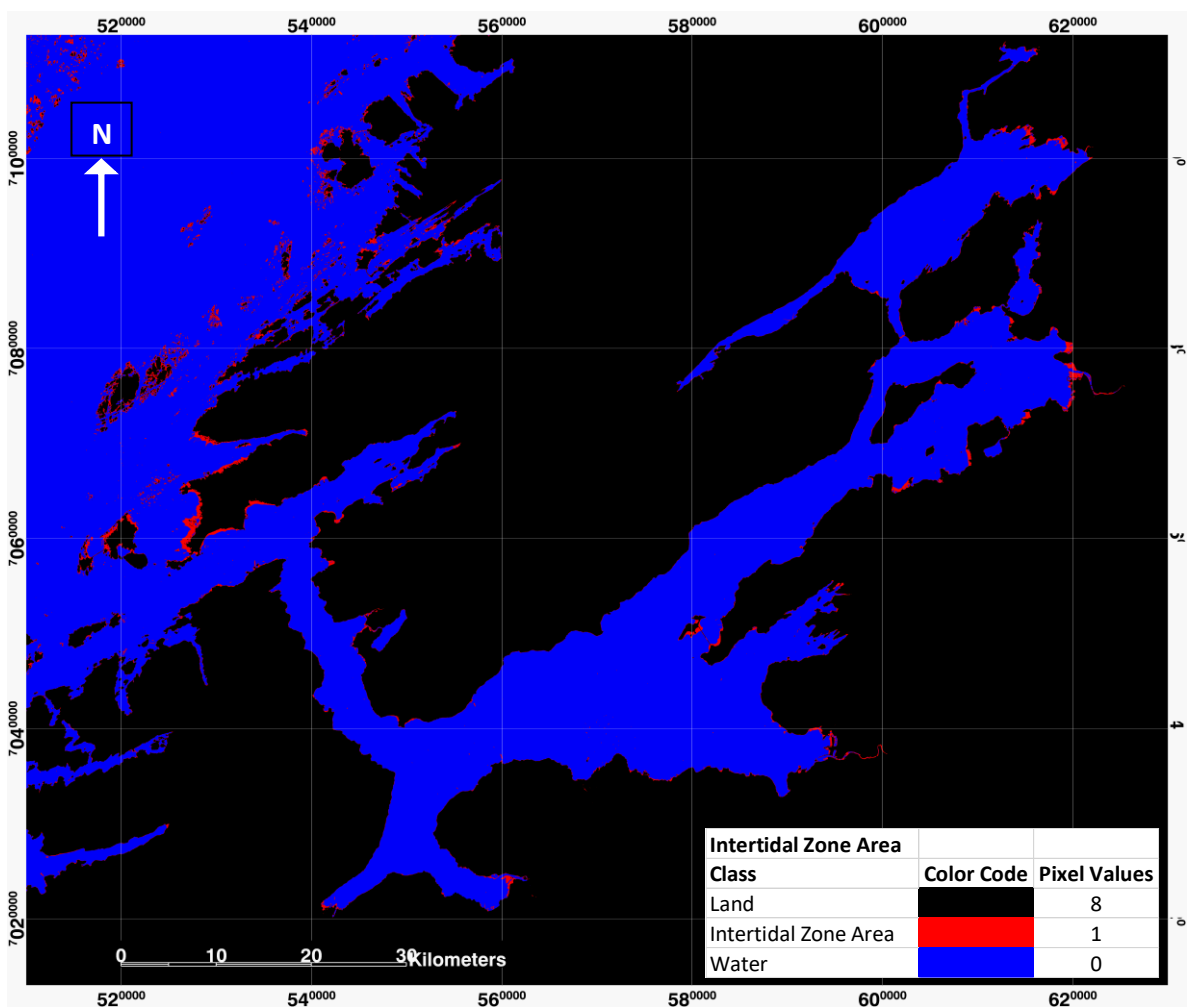


Figure 18. Final Sentinel-1 based Intertidal zone area (red) product in Trondheimsfjorden in UTM zone 32N

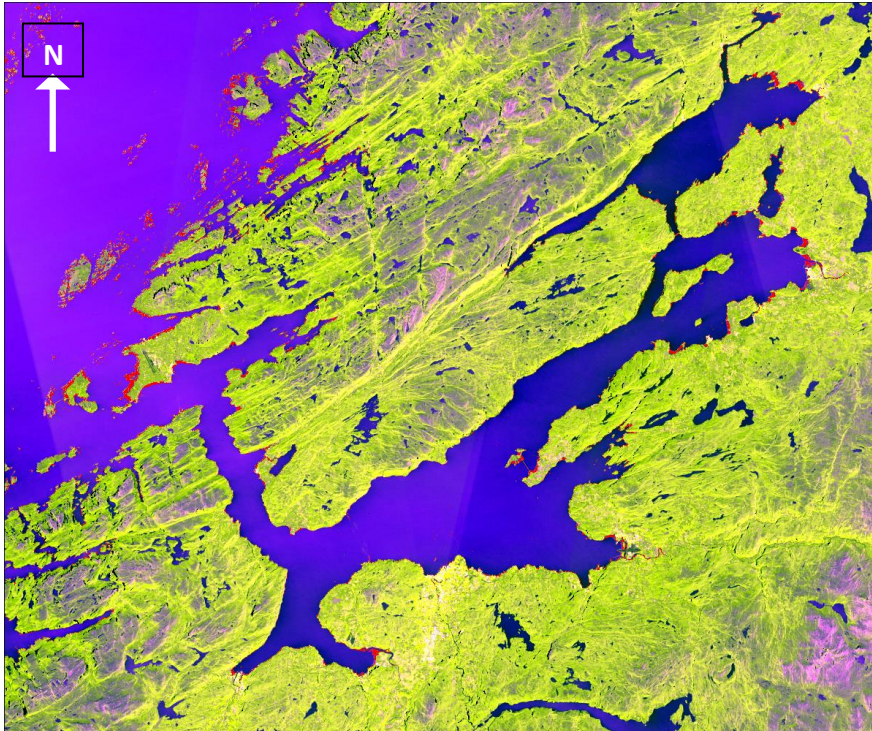


Figure 19. Intertidal zones in red detected by thresholding low and high backscatter percentiles.

Figure 20 shows the zoom-in areas around Grandefjære/Storfosna and the northeast of Trondheimsfjorden where large intertidal flats occur.

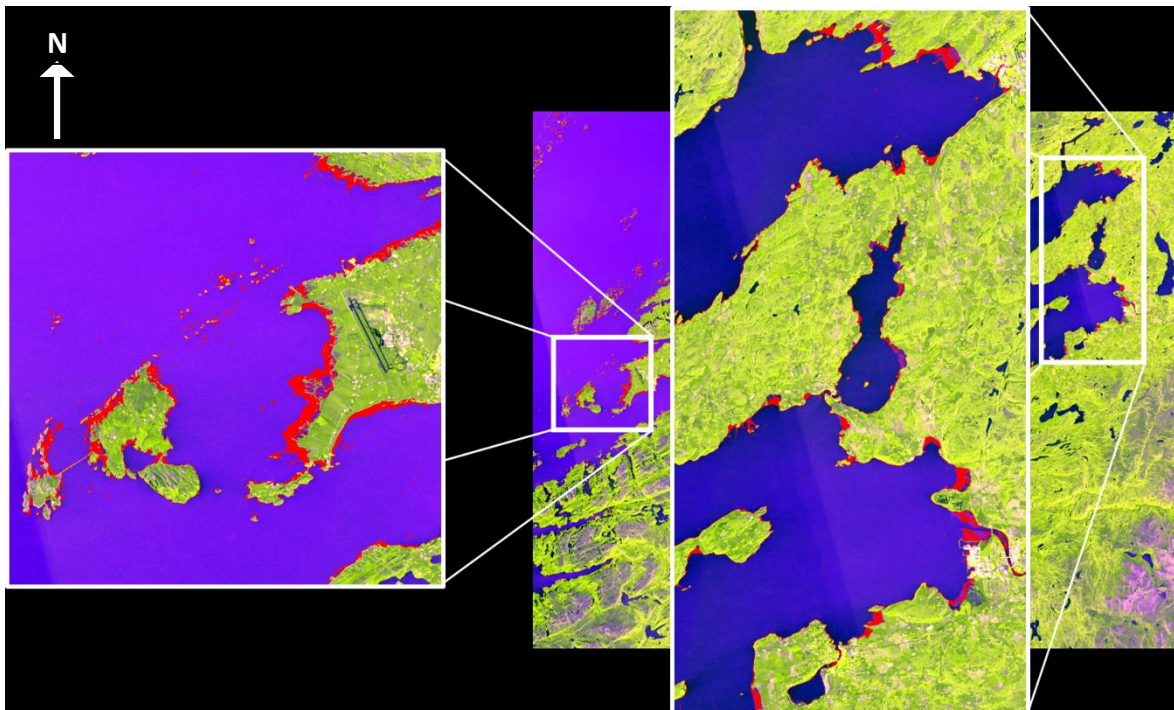


Figure 20. Zoom-ins of the intertidal zone results around Grandefjære/Storfosna and the northeast of Trondheimsfjorden.



Figure 21. Detected intertidal zone area (red) superimposed on an aerial image from Storfosna.



Figure 22. (Left) Minimum and (middle) maximum Sentinel-1 backscatter mosaics and (right) the detected intertidal zone area (red line) superimposed on an aerial image over Taura.

4.1.2 Mapping intertidal zones using Sentinel-2

Figure 23 shows the extent of the intertidal zones in Trondheimsfjorden as mapped using time series of Sentinel-2 data for 2018. Figure 24 shows the Grandefjære Ramsar site for more detail. In both figures, the zone that is mapped in red is interpreted to be the main intertidal zone. However, at many locations, this main intertidal zone is bordered by a zone (visually) interpreted by us to represent shallow water (see type mapping in 4.2.1; Figure 25). It is possible that the shallow water is actually part of the intertidal zone, and fieldwork or local knowledge is needed to better interpret this class. Figure 24 also shows the vector data from Naturbase indicating bløtbunnfjære (mudflats); according to the description, this dataset is based on visual interpretation and is manually digitised on screen. From Figure 24 and Figure 25 it is clear that the analyst included our shallow water class as part of the bløtbunn areas.

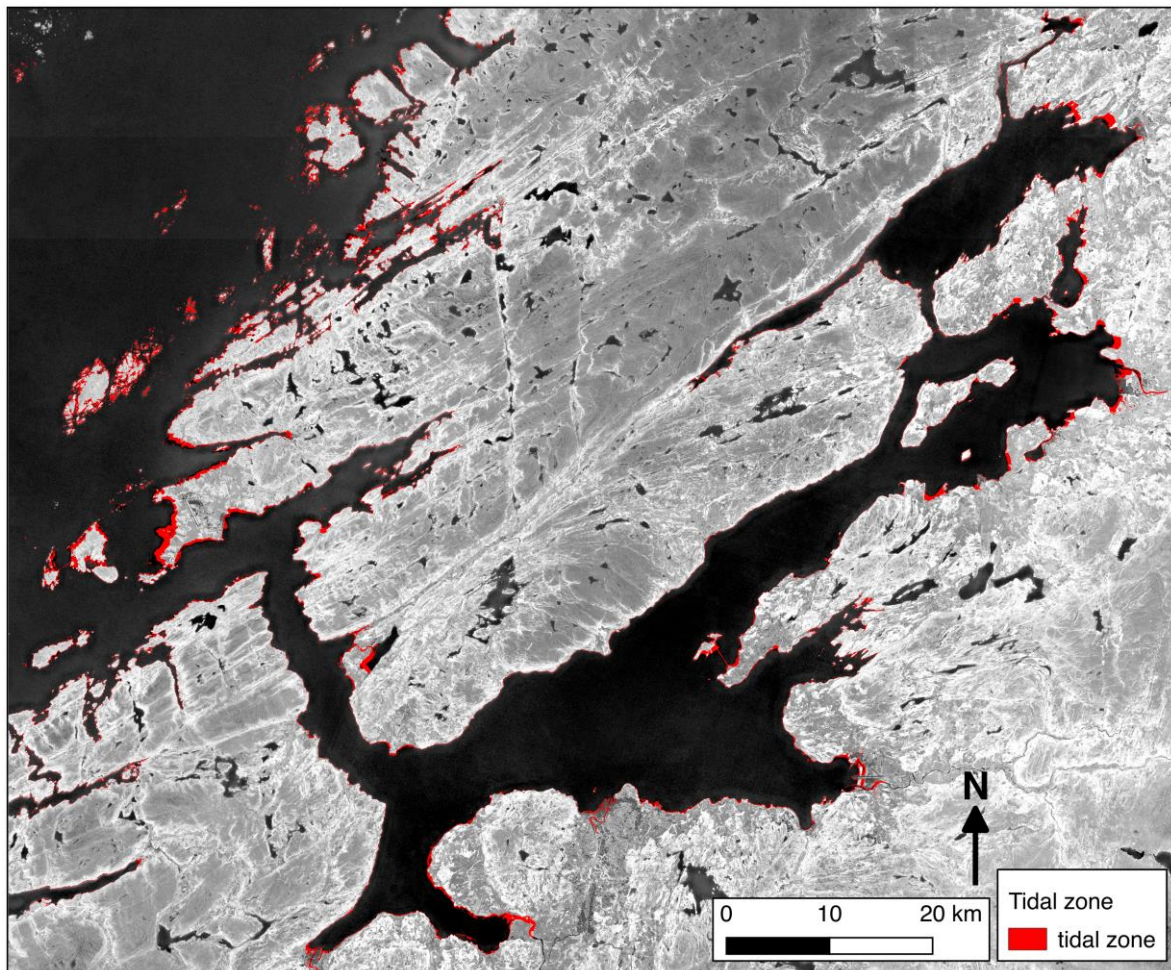


Figure 23. Intertidal zones indicated in red, plotted on an image showing the tndvi interval mean 10-90.

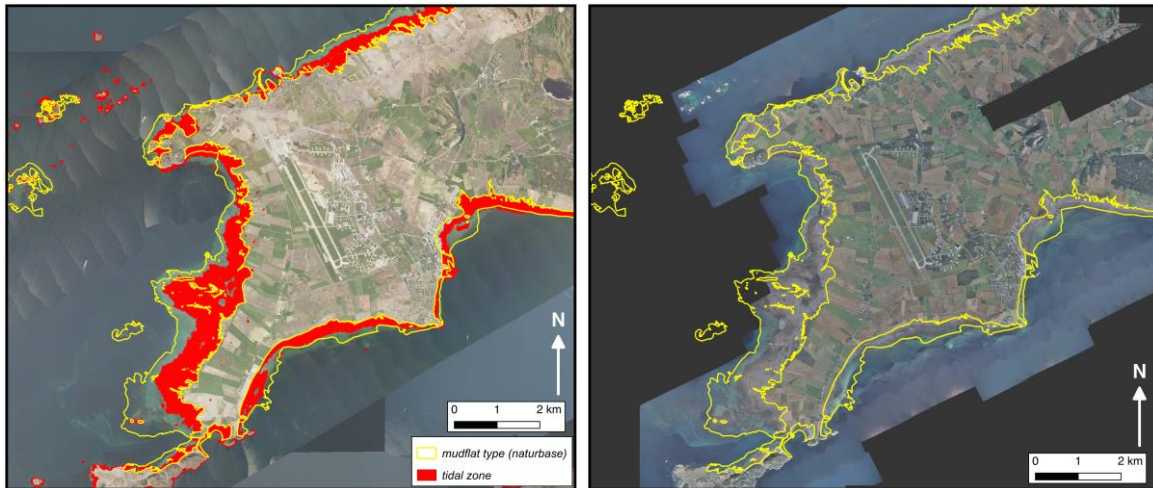


Figure 24. Detail of the extent of the intertidal zone of the Grandefjære site, as mapped by Sentinel-2 analysis. On the left, the intertidal zone is plotted in red on an aerial photo, with the bløtbunn (mudflat) vector data from Naturbase indicated by a yellow line. On the right, aerial photos at low tide (2010) with the bløtbunn dataset from Naturbase.

4.2 Intertidal Zone Type Mapping

4.2.1 Mapping intertidal ecosystems using Sentinel-2

Figure 25 and Figure 26 show 2 examples of the details that can be mapped within the intertidal zones. Based on visual comparison with available aerial photos taken at relatively low tide (from 2010), it is interpreted that we can distinguish mudflats, zones with seaweed and other vegetation within the intertidal zone, rocky outcrops within the intertidal zone, intertidal pools, zones with shallow water which may include (partially) submerged seaweed, possibly sandy/pebbly beaches, and mixed pixels, which include narrow rocky coastlines (mixture of rock and water).

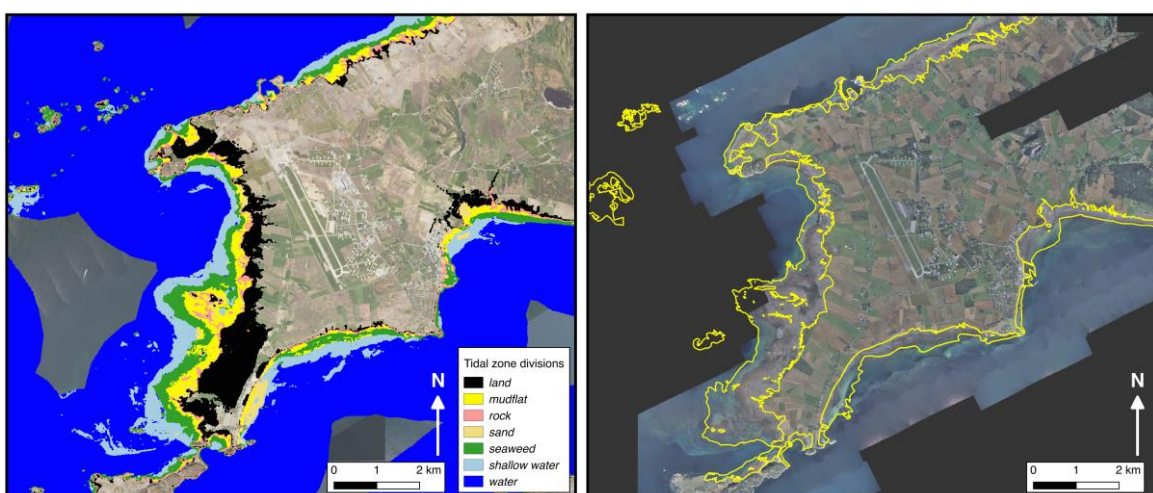


Figure 25. Details within the intertidal zone of the Grandefjære Ramsar site. Left: 7 classes identified within, and adjacent to, the intertidal zone, plotted on an aerial photo. Only the area in the coastal mask is classified. Right: aerial photo with lowest tidal level available (2010) from Norge i Bilder, overlain by the bløtbunn vector data in yellow, for visual comparison.

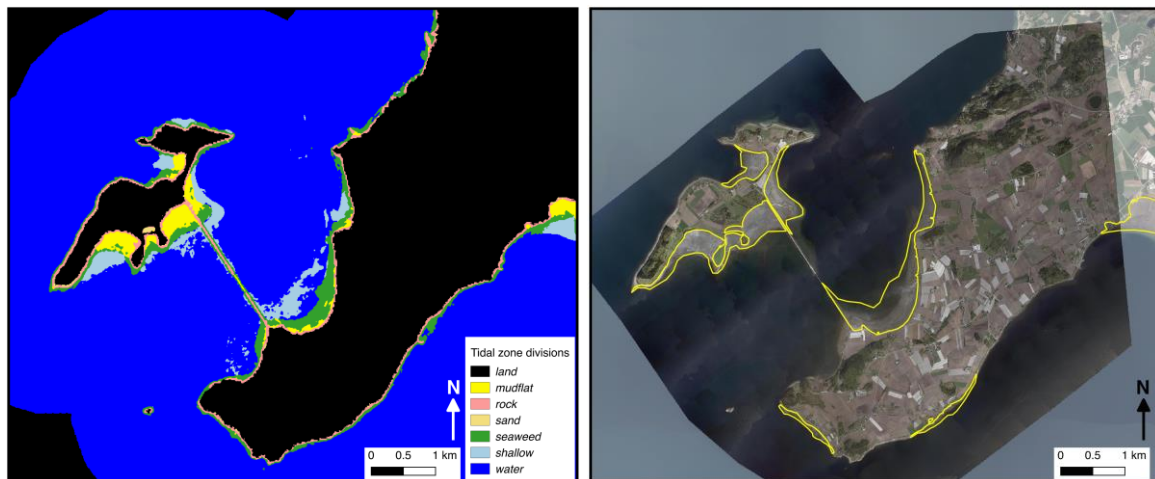


Figure 26. Details within the intertidal zone of the Tautra Ramsar site. Left: 7 classes identified within, and adjacent to, the intertidal zone, GMM segmentation. Right: aerial photo with lowest tidal level available (2009) from Norge-i-Bilder, overlain by the bløtbunn vector data in yellow, for visual comparison.

4.2.2 Intertidal Zone Type from Sentinel-1

The final result of the intertidal zone type map based on the MLH classification using all percentile images of VV and VH polarizations is shown in Figure 27. Figure 28 compares the results of the MLH and NN classifications using all percentile images as feature and only the 98% percentile image and compares them to the aerial image.

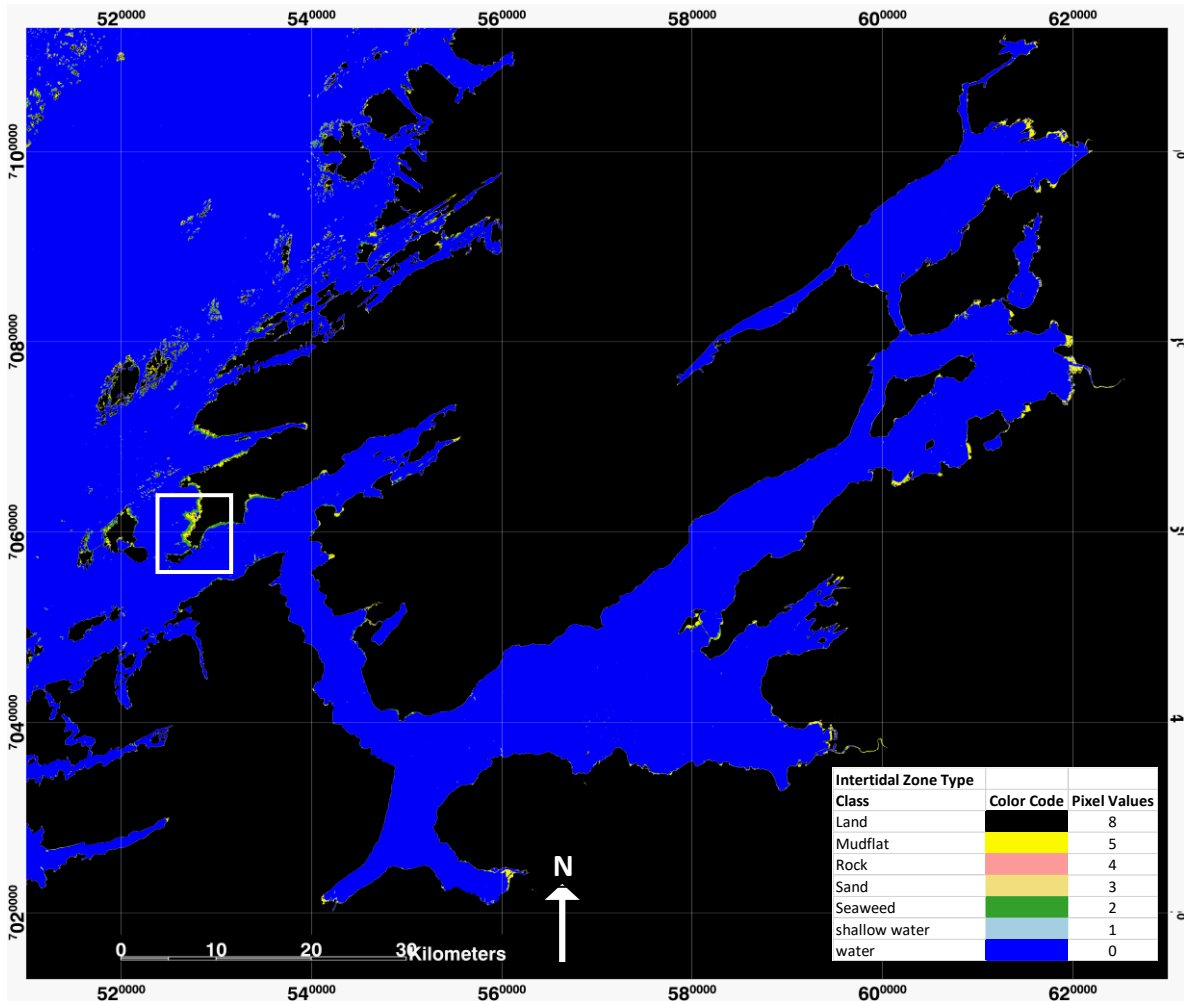


Figure 27. Final intertidal zone type based on Sentinel-1 2017-2018 data of Trondheimsfjorden using an MLH classification with all percentile images.

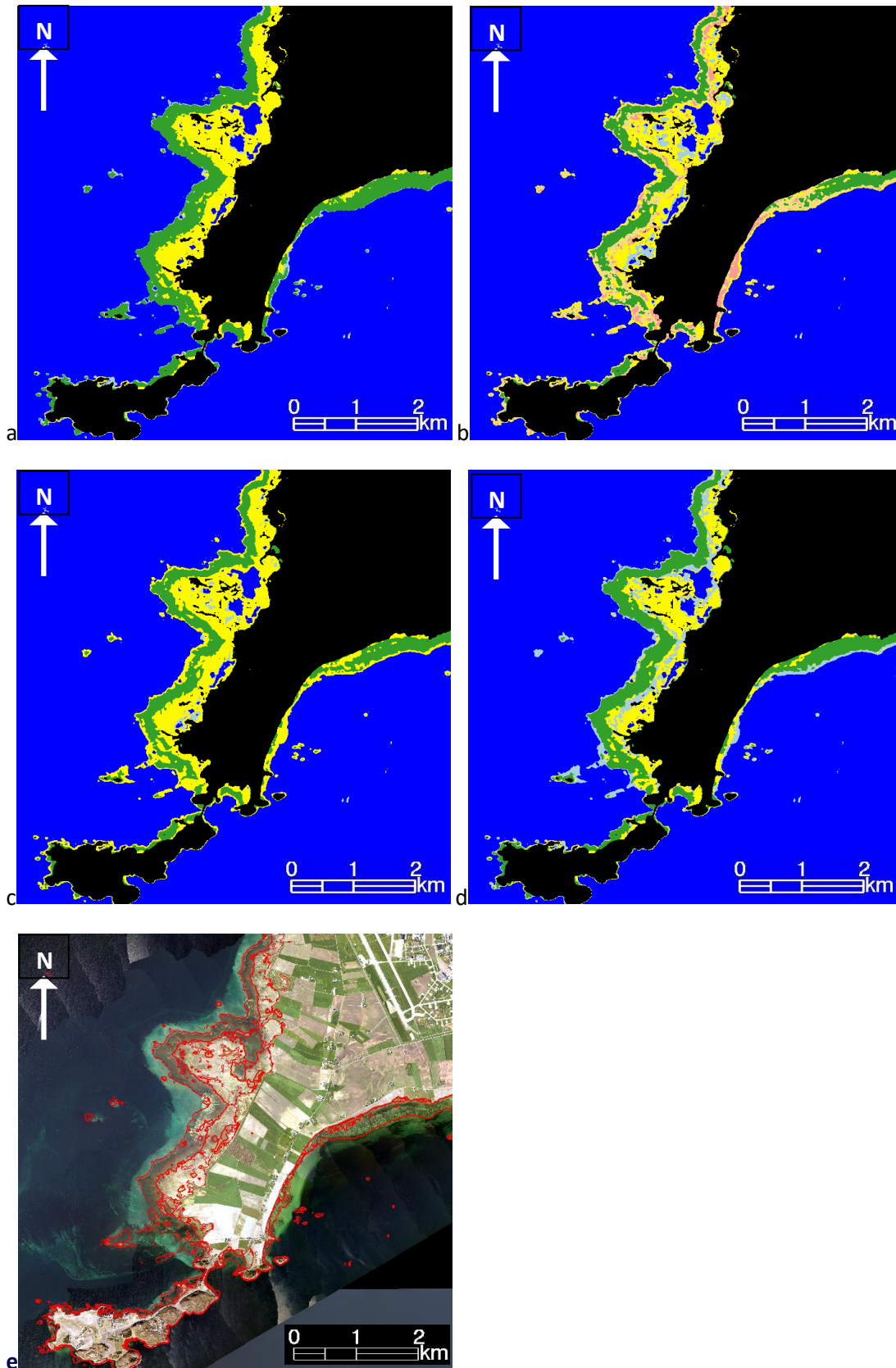


Figure 28. Zoom-in on Grandefjære of the type classification using MLH on (a) all percentile images, (b) on the 98% percentile VV and VH images, and using NN on (c) all percentile images, (d) on the 98% percentile VV and VH images. (e) is the aerial image as reference.

4.3 Mapping of atmospheric exposure with Sentinel-1

The final result of the intertidal zone atmospheric exposure product (ITZ_AtmosExp) based on Sentinel-1 using the whole 2017-2018 time series over Trondheimsfjorden using the method described in section 3.3 is shown in Figure 29. Figure 30 and Figure 31 show zoom-ins of the white rectangles.

The land mask area from S1 in brown is the area up to 50 cm above sea level in the 10m Norwegian DEM and is in theory the area that might be affected by sea level rise of 50cm.

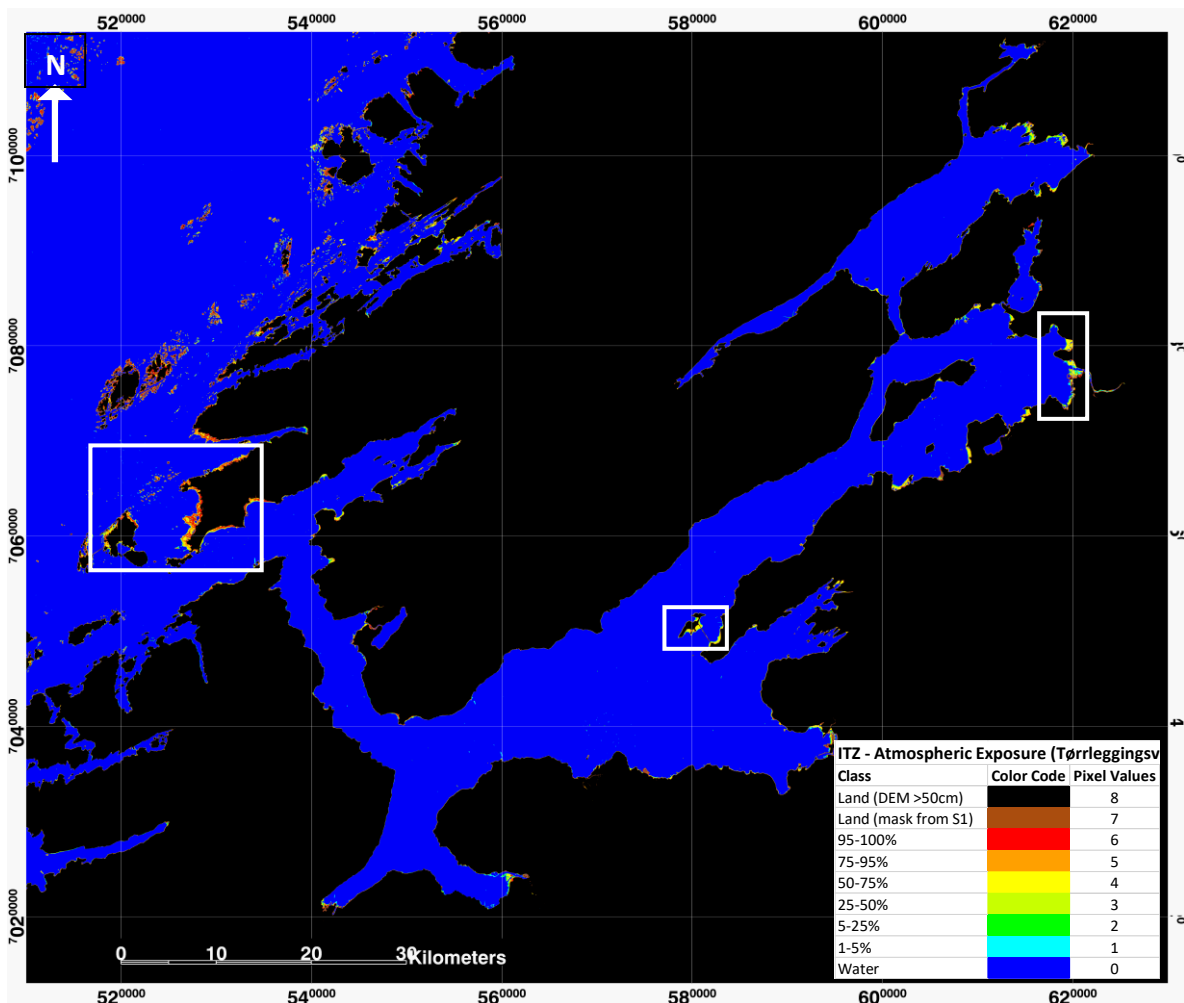


Figure 29. Final intertidal zone atmospheric exposure product based on Sentinel-1 2017-2018 data of Trondheimsfjorden.

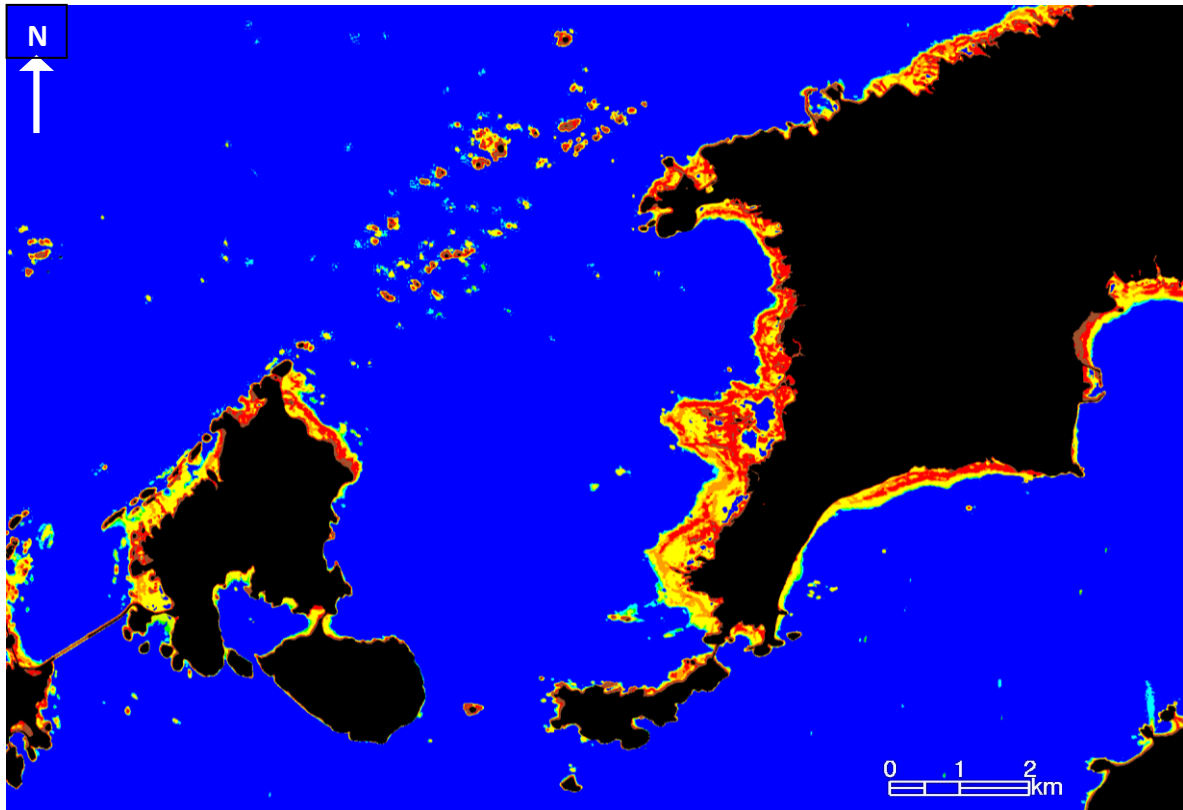


Figure 30. Zoom-in of the ITZ_AtmosExp around Grandefjære and Storfosna at the exit of Trondheimsfjorden in the west.

ITZ - Atmospheric Exposure (Tørrleggingssv)	Color Code	Pixel Values
Land (DEM >50cm)	Black	8
Land (mask from S1)	Brown	7
95-100%	Red	6
75-95%	Orange	5
50-75%	Yellow	4
25-50%	Light Green	3
5-25%	Green	2
1-5%	Cyan	1
Water	Blue	0

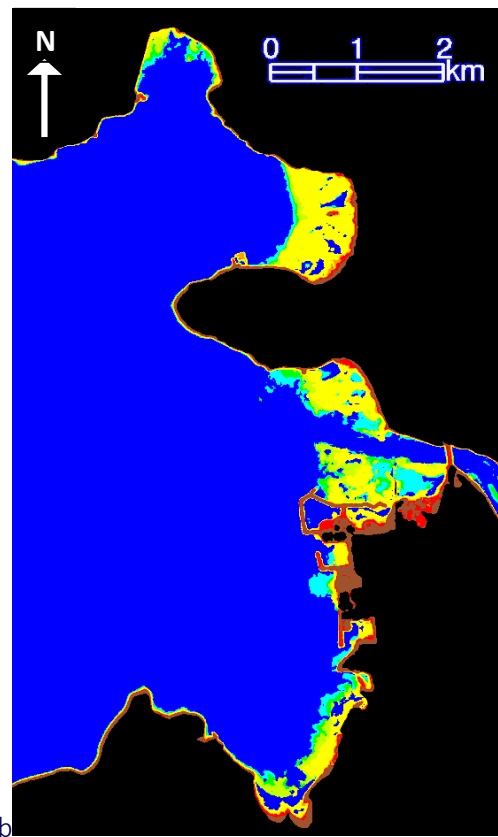
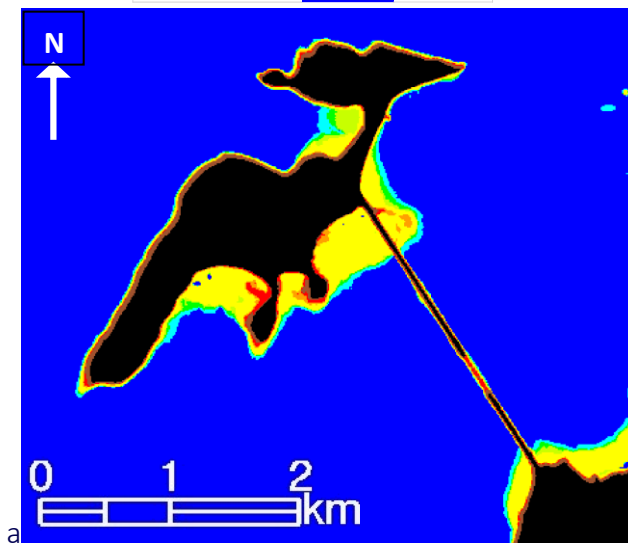


Figure 31. Zoom-in of the ITZ_AtmosExp around (a) Tautra island and (b) Kausmo fjære/Verdal.

4.4 Mapping changes in the intertidal zone.

Figure 32 and Figure 33 show examples of detected changes by thresholding the difference of the 95 percentile images from 2017 and 2018.

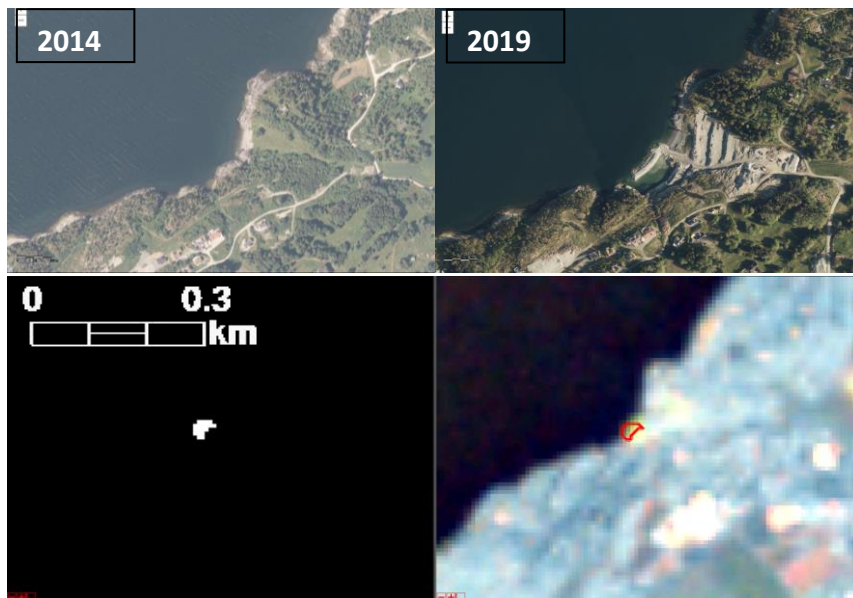


Figure 32. Detected establishment of a new sand mine at Småtta close to Vigtil. (Upper left) aerial photo from 16 Sep 2014, (Upper right) aerial photo from 17 May 2019, (Lower left) change detected from S1 between 2017 and 2018, (lower right) S1 averaged mosaic 2018.

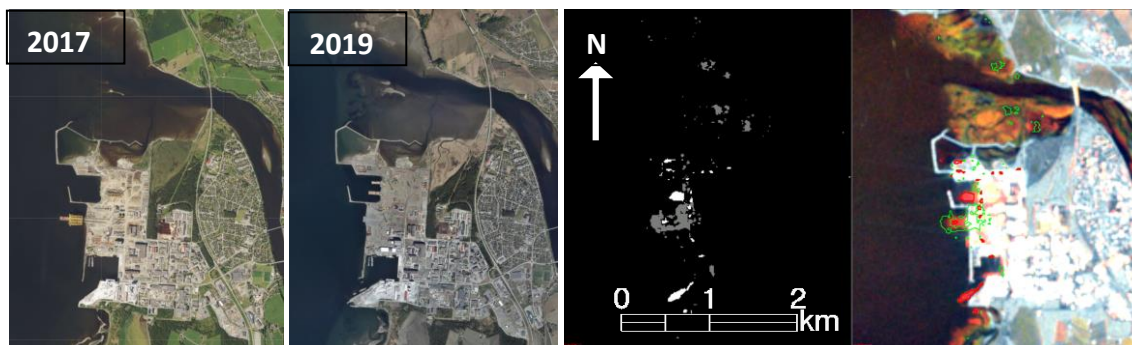


Figure 33. Detected changes in the harbour of Verdal from 2017 to 2018 by thresholding the difference of the 95% percentile images from both years. The aerial images date from 30 June 2017 and 17 May 2019.

5. Accuracy Assessment

5.1 Field validation

As aerial mosaics come without an exact time stamp, the only possibility to assess the accuracy of the detected intertidal zone extent was by collecting ground data by GPS tracking along the water line at low tide condition. This was done at Lille Grindøya, close to Tromsø on 19 July 2019 (Figure 34). Figure 35 and Figure 36 show a zoom of Figure 34 together with the intertidal zone area and intertidal zone atmospheric exposure product. The original 20m resolution results from Sentinel-1 has been sub-sampled by cubic convolution on a 1m resolution grid with the aerial data.

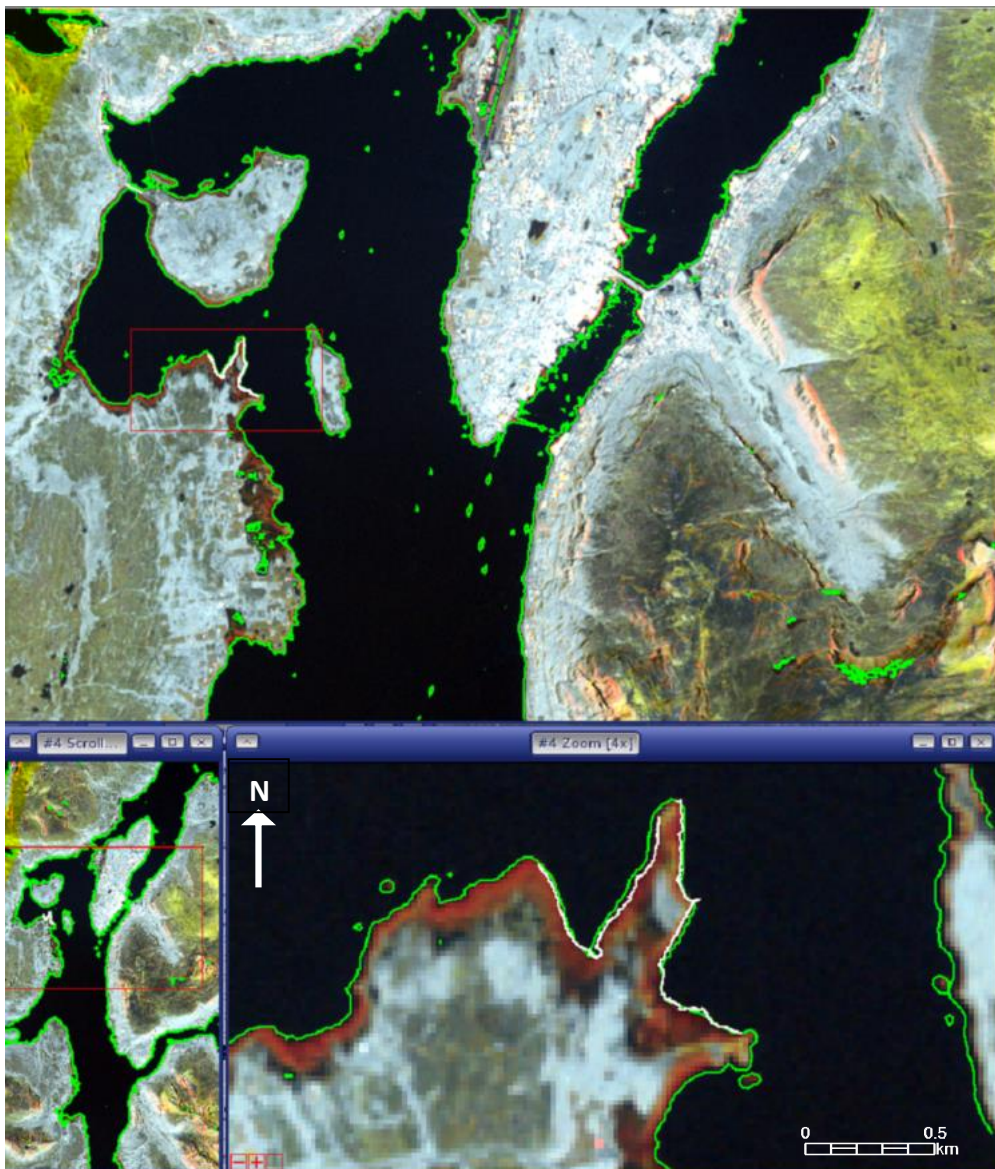


Figure 34. Field site Lille Grindøya close to Tromsø. The image composite shows a combination of VH percentiles in RGB=[95, 50, 5]. The intertidal zone is in red. The white line shows the GPS track from walking along the waterline. The green line shows the Contour line of -20.5dB of the 95%ile.

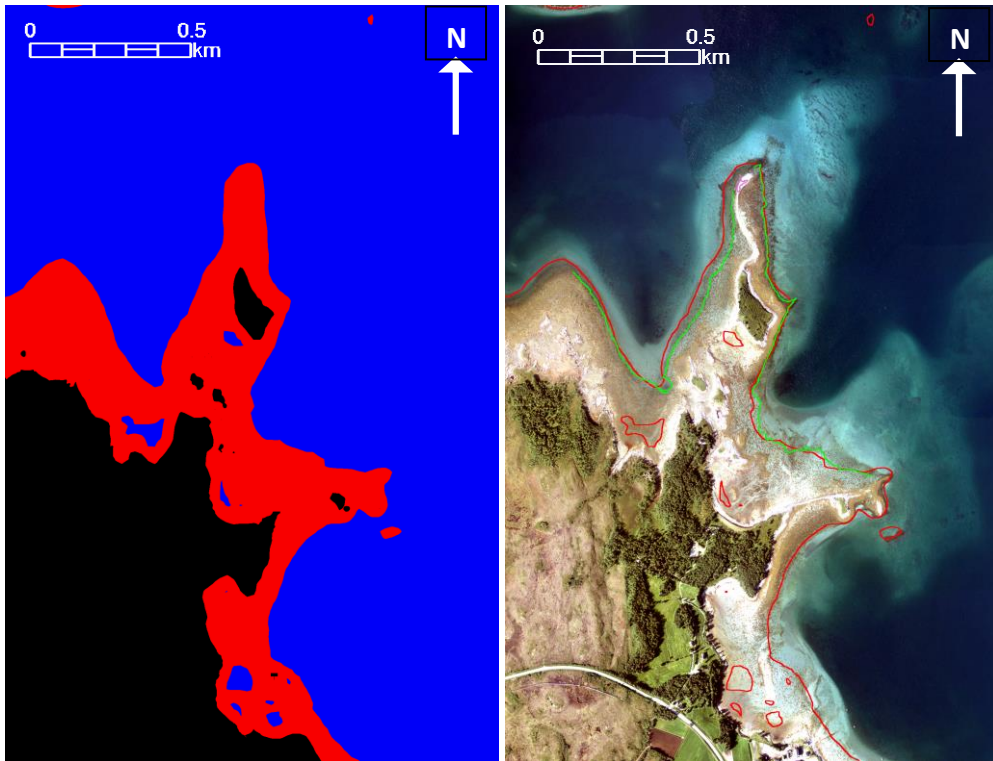


Figure 35. Zoom-in of Figure 34 on Lille Grindøy. The green line shows the GPS track from walking along the waterline around high tide on 19 July 2019. The red line shows the maximum extent of the intertidal zone area measured with the proposed method with Sentinel-1.

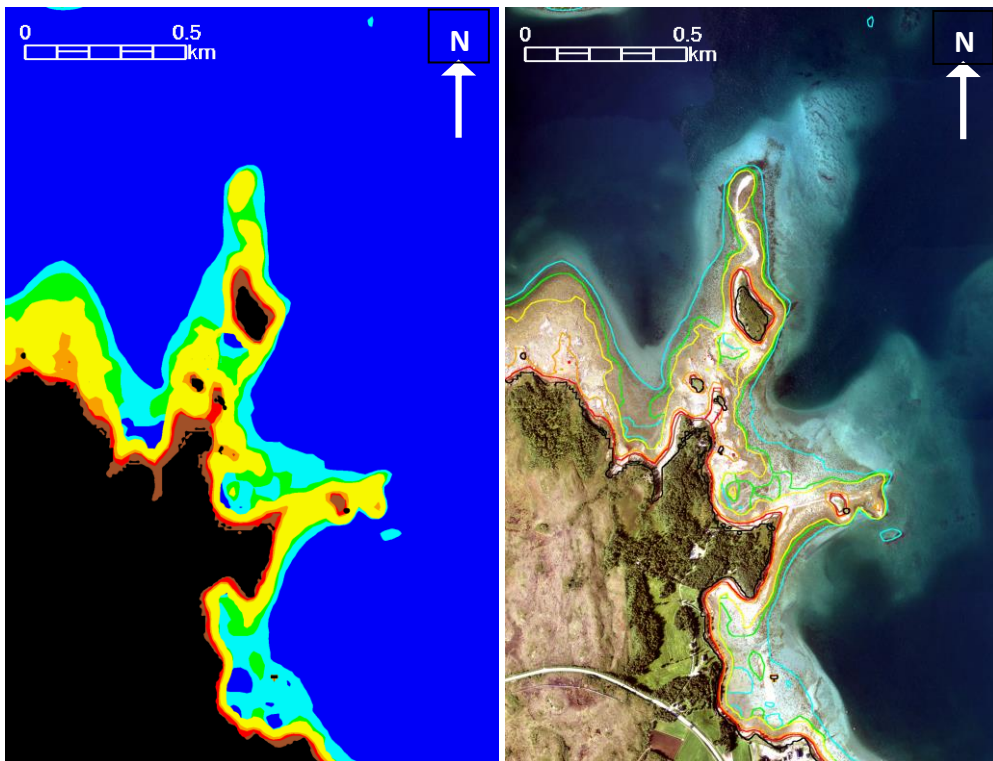


Figure 36. Zoom-in of Figure 34 on Lille Grindøya. The coloured lines show line of different percentages of atmospheric exposure. line shows the GPS track from walking along the waterline. The green line shows the Contour line of -20.5dB of the 95%ile.

Figure 37 and Figure 38 show contour line of the 95 percentile and 5 percent VH backscatter images in the range of -21dB to -16 dB and 25db to -19 dB, respectively, showing how robust the water-land discrimination is with simple thresholding.

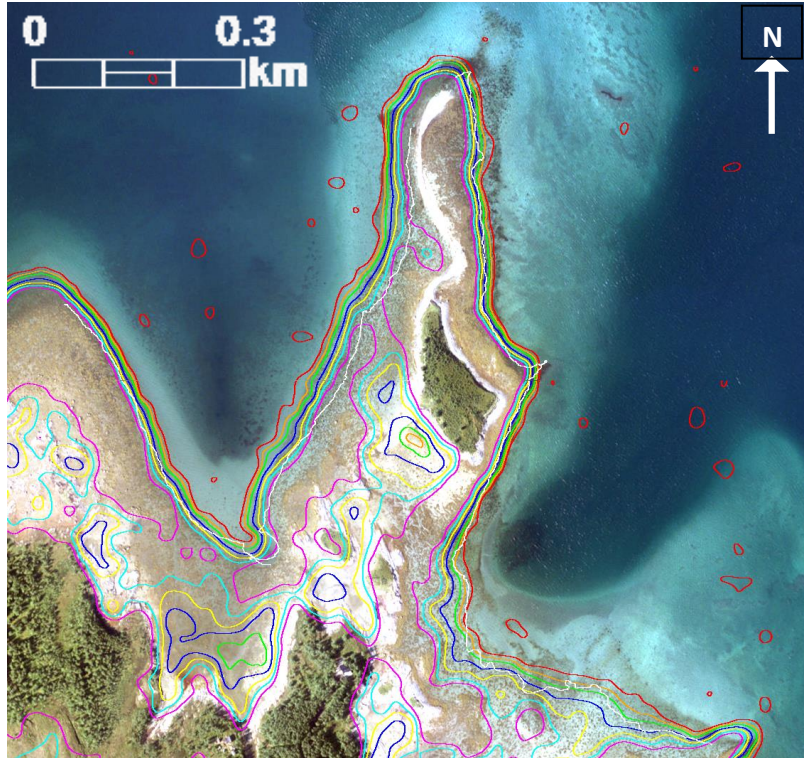


Figure 37. Applying different thresholds on the 95-percentile image. Threshold var from -21 dB to -16 dB. The orange line is a threshold of -20.5dB.

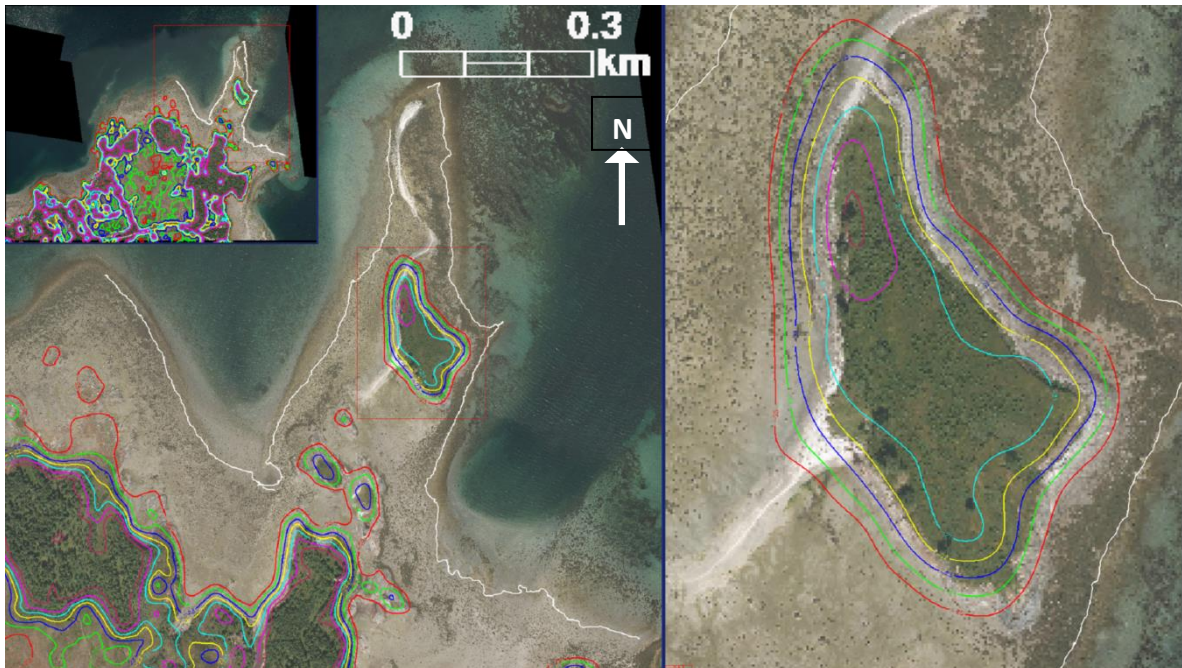


Figure 38. Thresholding of the 5% percentile for the high-tide water line, i.e. land detection with VH backscatter thresholds varying from -25dB to -19dB

5.2 Inter-comparison between Sentinel-1 and Sentinel-2 results

Overall, the independent results based on Sentinel-1 and Sentinel-2 seem to be consistent and in good agreement. Figure 39 compares the results in detail around Grandefjæra and Tautra. Some important observations:

- The mudflat and seaweed classes are in relatively good agreement and are the dominant classes of the intertidal zone.
- Rocks and sand occur only locally and might be underrepresented in Sentinel-1. The main reason is that training polygons of this class were very small and most of them were outside of the defined S1 intertidal zone.
- Shallow water does rarely occur in the S1 classification, which is quite logic as, Sentinel-1 will not see beyond the water surface.
- The intertidal zone area detected by Sentinel-1 seems to be slightly bigger than the Sentinel-2 (excluding the shallow water).

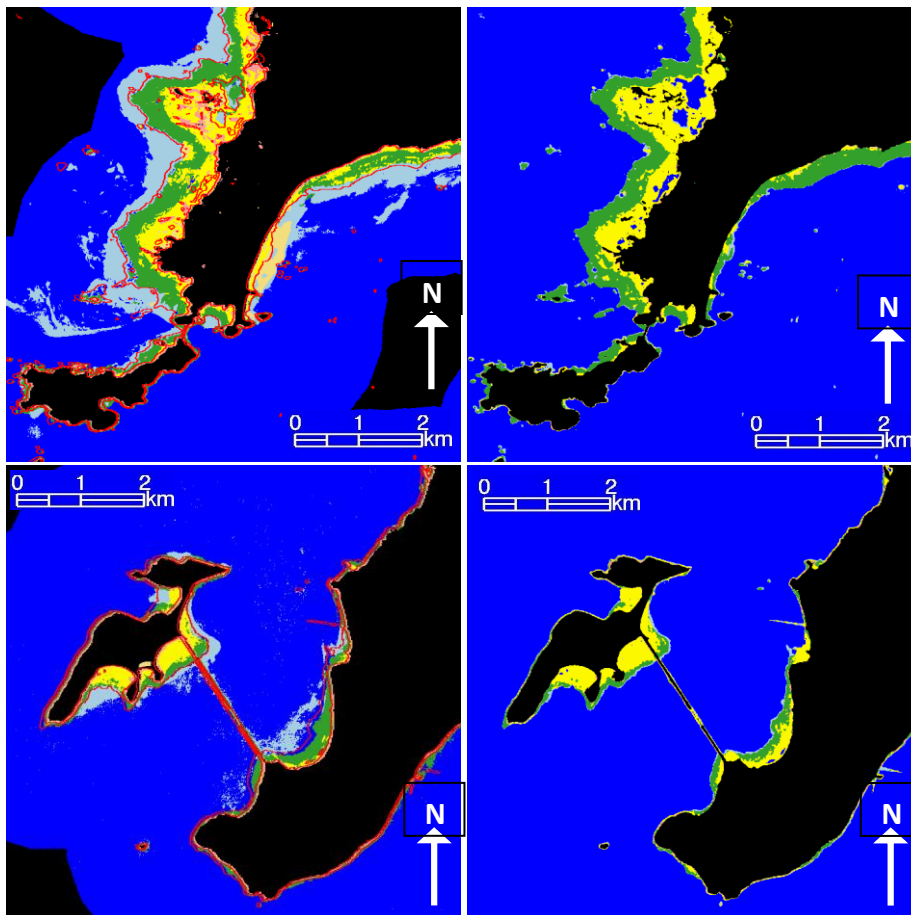


Figure 39. Inter-comparison between S2 (left panels) and S1 (right panels) results around Grandefjæra (upper panels) and Tautra (lower panels)

6. Conclusion

The study shows that both Sentinel-1 and Sentinel-2 are well suited to map the intertidal zone when using very long time series to capture all states of the intertidal zone and different tidal levels. Results were as expected or even beyond expectations. Sentinel-1 has the advantage that every acquisition is usable as it is not dependent on clear sky conditions and therefore the potential of acquiring the highest and lowest spring tides is therefore higher. The slightly bigger intertidal zone detected with Sentinel-1 confirms this.

Also, intertidal zone type mapping of both satellites, at least considering the mudflat and seaweed classes, are in good agreement. Other classes like sand and rock should be identifiable, probably better with Sentinel-2 than Sentinel-1, but as these classes are underrepresented, the training data may not have been enough, especially as most of them lie outside of the intertidal zone detected by Sentinel-1. However, one should not forget the Sentinel-1 and Sentinel-2 detect different parameters:

Optical sensors have the ability to see through clear water which means that:

- Optical data can detect shallow waters but might not always be able to detect the exact water line. Similarly, it has been proven difficult to identify the exact waterline from aerial photographs from Norge-i-Bilder. Ground truth (field data) at low tides is therefore needed to assess the accuracy of the interpretation.
- The presence of suspended sediments from river outflows and along the coast can cause misclassification in Sentinel-2 data.

On the other hand, Sentinel-1 data is very sensitive to water, meaning that:

- Ponds, even very shallow ponds, inside the intertidal zone show up as water in Sentinel-1 images.
- Very wet and water-saturated surface might still have backscatter signatures below the threshold.

These assumptions need to be confirmed with field observation and the overall definition of the intertidal zone might need to be reviewed. From field observation around Lille Grindøya in Troms, it was also quite clear that the water line is rarely a clear line in shallow waters and small topographic features like small rocks, seaweed at the surface in shallow water and sand banks are challenging examples for a simple intertidal zone definition of surfaces being covered by water at high tides.

It turned out to be challenging to interpret aerial photos, particularly to distinguish between areas that are probably always covered with (very) shallow water and those that get exposed at low tides. The mudflat bløtbunn vector data from Miljødirektoratets Naturbase appear to include shallow waters in some areas and not in others. An additional complication is that the exact acquisition time of aerial photos is unknown and that the photos are unlikely taken at the lowest tides. The aerial photo data base has inhomogeneous quality and lightning conditions, which makes it nearly impossible to use them for national wide mapping. They can be used for some validation of vegetation occurrence, but field data will be crucial for a real accuracy assessment of

the intertidal zone extent, as well as being necessary to help learn how to identify various classes in the aerial photos, such as like mudflats and sand.

The Copernicus Land Monitoring Service (CLMS) in cooperation with the Copernicus Marine Environment Monitoring Service (CMEMS) is working on a comprehensive coastal zone monitoring solution that can address the complex and dynamic situations found in coastal environments. "Intertidal flats" (7.2.3.) is a subcategory under "coastal water (7.2)" under "wetlands" defined as "Generally un-vegetated expanses of mud, sand or rock lying between high and low water marks; area between tide marks, basically composed by mud, rocks or boulders." (Copernicus)

The first delivery of these Coastal Zones products is expected by the end of 2020 and could be compared to the national products. In view of the crude definition above, we do not expect that such products will contribute more information to the methods presented here. However, we expect our methods to work also in central Europe, probably with longer integration periods because of lower satellite coverage and could therefore contribute also to the Copernicus efforts. The CLMS and CMEMS teams could be contacted for a possible cooperation.

7. Recommendations

7.1 National Intertidal-zone mapping

Processing the Trondheimsfjorden area in this study was based on the whole data set of 2017 and 2018, which for Sentinel-1 means over 900 acquisitions and therefor 2-3 terabyte of data.

Somewhat less for Sentinel-2 data as scenes with high cloud cover percentage are filtered out prior to further processing. The main challenges with extending the intertidal zone mapping to a national scale is therefore the handling of large amounts of data. There is therefore a need to take the method to the data, and processing all of Norway should therefore be done in the cloud.

There are mainly three options to do so:

- The Google Earth Engine (GEE)
- One of the Copernicus Data and Information Access Services (DIAS)
- A national ground segment that provides the data as well as processing capabilities.

GEE:

GEE is a cloud-based platform for the analysis of geospatial data, supporting both java script and python as programming languages, and includes a public data archive of satellite images. The data archive includes Landsat images going back to 1972, Sentinel-2 and Sentinel-1 products, which facilitates the analysis of large datasets. In principal, GEE is free for research, education and non-commercial applications, but it would need to be confirmed with Google if this includes government applications. Exporting and downloading the end products of the analysis may, however, be subject to a cost depending on the size of the product. As GEE is a service developed by Google, a commercial operator, there are no guarantees that access will always remain free.

The workflow for the processing of Sentinel-2 data has already been developed on GEE using java script and can be therefore theoretically be adjusted easily to a nationwide scale. However, there are several issues which may cause complications and will need to be investigated:

1. as the mapping is based on the analysis of time series, mapping on a national scale will require the handling of large amounts of data. This may cause issues with user memory allocations, and possible limitations to the export of end products. Solutions to this, such as more efficient coding and/or potentially dividing up in smaller tiles, may need to be investigated. For Trondheimsfjorden, the processing code takes a few minutes to run, and the exporting of results 10-20 minutes.

2. Norway has a long coastline stretching from latitudes 57° to 71°; this range in latitudes means that there will be variations in the sun angle, variations in weather and water conditions (e.g. ice cover), variations in vegetation. Even though the Sentinel-2 level 2-A products have been corrected for sun angle, there may still differences that effect the classification.

3. The cloud masking procedure is not perfect. It would be useful to investigate other cloud masking algorithms to see which algorithm performs best across all of Norway.

Sentinel-1 data is available also on GEE, but only as pre-processed data and we need to investigate if this also includes auxiliary data from the preprocessing like incidence angle and topographic induced shadow and over lay mask. We assume that processing on GEE would be possible, but codes would need to be transferred into this system. However, at this point extracting the data to make it available outside GEE might be challenging.

DIAS:

NORCE has successfully tested similar Sentinel-1 data processing on CREODIAS for other projects. We expect that it is technically feasible and maybe the easiest to transfer the current python processing workflow for Sentinel-1 to CREODIAS. However, the use of CREODIAS for processing is also subject to costs dependent on data storage, processing machine use performance and thereby probably also on the speed of processing.

National Ground Segment (NGS)

It seems that there has been some effort to provide pre-processed Sentinel data over Norway through an NGS, but at this time, we are unaware of the situation, format of the pre-processed data and functionality of the system for cloud processing. Our impression is, that the NGS is still under development and unlikely to be considered as a solution in the short term.

In-house processing:

As a last option, it is of course also possible to process the data in-house, but data download and processing might be challenging on an operational basis in the future.

The above options need to be investigated further before advancing with nation-wide processing considering also the priorities of MD.

7.2 Accuracy assessment

This study has shown that aerial imagery from Norge-i-Bilder does not give us enough information on the highest and lowest water line as explained in the text. To better understand the limitations of our results, correctly parametrize and train the models and classification algorithm to build training polygons, we suggest having a field campaign over the current study area

Trondheimsfjorden. During this study and in the results, we have distinguished specific regions that would be necessary to visit. Some important questions that need clarification are:

- The exact position of the highest and lowest water line in areas with wide intertidal zones, mainly on the east side of the fjord and around Grandefjære and Storfosna.
- The position of the water line corresponding to different percentile thresholds to assess the accuracy of the atmospheric exposure product.
- Mapping specific areas of sand and rocks and distinguish them from mudflats.
- Compare aerial photos with conditions on the ground to learn how to distinguish the different types of tidal zones from the aerial photos. Interpretation of aerial photos will be crucial in order to generate a database of training and validation data on a national scale.
- Are water pools inside the intertidal zone really water pools or water saturated grounds?

We suggest a 1-2 weeks field work in this area to visit the above sites. The visit to each site should contain at least the low and high tide timing and last at least a half tidal cycle (>6h) to capture all the different states. The date of such a visit should also occur during a spring tide period.

A final national product would also need some kind of accuracy assessment in the field, and we suggest doing this at least at three locations, so in addition to Trondheimsfjorden, one location in southern and one in northern Norway.

7.3 Proposal for nationwide mapping

1. Develop a nationwide database with training and validation data based on the interpretation of aerial photos available in Norge-i-Bilder. This can be a combination of training polygons and random points, but all classes need to be sufficiently represented. Random points can be generated stratified by class based on a classified image to ensure sufficient representation of all classes, and manually interpreted against aerial photos to create a validation database. Interpretation of aerial photos is subject to learning to distinguish different types from fieldwork, as described in 7.2. *Ca 1 month (2 weeks for 2 analysts).*

2. Collection of ground truth data to map the extent of the tidal zones by mapping the water line at very low and high tides using a GPS. At the same time, the position of the waterline can be mapped by GPS at intermediate stages of the tidal cycle to assess the accuracy of the atmospheric exposure. *Fieldwork in Trondheimsfjorden, 1-2 week; Tromsø, ca 2 days; southern Norway, ca 3-5 days.*

3. Apply the GEE code for the processing of Sentinel-2 data to all of Norway, check and validate the results and modify the script if necessary. Test different cloud masking methods. Accuracy assessment using the database proposed in 7.3.1.

4. Operationalize the Sentinel-1 workflow in python as most of the development have been made manually during the first phase of the project.

5. Implement the python workflow for the processing of Sentinel-1 data on one of the cloud-based services.

6. Identify the strengths and weaknesses of Sentinel-1 and Sentinel-2 for the mapping of intertidal zones based on the accuracy assessments and design a method of combining the 2 datasets.

8. Project limitation

The total budget of this project is limited, and we estimate an overuse of funding of about 50% during the first phase already. Considering the vast amount of data for processing and the workload of developing the methods, operationalizing the methods for extending the methods for nation-wide mapping and provide quality checked products, some priorities must be agreed on during the next phase of the project.

9. Acknowledgments

The authors wish to thank our colleagues at NORCE that have developed that SAR processing line and continuously improve it with adding new tools.

10. References

Copernicus Land Monitoring Service. Coastal Zones Production of Very High Resolution Land Cover/Land Use dataset for coastal zones of the reference years 2012 and 2018. Nomenclature Guideline. <https://land.copernicus.eu/user-corner/technical-library/coastal-zone-monitoring>

Copernicus. http://coastal.planetek.it/geocommunity/dwnld/CZ_Guideline.pdf

Davidson, N.C., and Finlayson, C.M., 2019. Updating global coastal wetland areas presented in Davidson and Finlayson (2018). *Marine and Freshwater Research*. Doi: 10.1071/MF19010.

Delegido, J., J. Verrelst, L. Alonso, J. Moreno. Evaluation of Sentinel-2 Red-Edge Bands for Empirical Estimation of Green LAI and Chlorophyll Content. *Sensors* 2011, 11, 7063-7081.

ESA, Sentinel Success Stories, https://sentinel.esa.int/web/sentinel/news/success-stories/-/asset_publisher/3H6l2SEVD9Fc/content/copernicus-sentinel-1-supports-detection-of-shoreline-positions?redirect=https%3A%2F%2Fsentinel.esa.int%2Fweb%2Fsentinel%2Fnews%2Fsuccess-stories%3Fp_p_id%3D101_INSTANCE_3H6l2SEVD9Fc%26p_p_lifecycle%3D0%26p_p_state%3Dnormal%26p_p_mode%3Dview%26p_p_col_id%3Dcolumn-1%26p_p_col_pos%3D1%26p_p_col_count%3D2

Gilvear, D., Tyler, A., and Davids, C., 2004. Detection of Estuarine and Tidal River Hydromorphology Using Hyper-Spectral and Lidar Data: Forth Estuary. *Estuarine Coastal and Shelf Science*, 61: 379-392. Doi: 10.1016/j.ecss.2004.06.007

Gorelick, N., Hancher, M., Dixon, M., Ilyushchenko, S., Thau, D., & Moore, R., 2017. Google Earth Engine: Planetary-scale geospatial analysis for everyone. *Remote Sensing of Environment*, 202: 18-27. Doi: 10.1016/j.rse.2017.06.031.

Haarpaintner, J., B. Killough, R. Mathieu, L. Mane, B. Gessesse Awoke (2019). Advanced Sentinel-1 Analysis Ready Data for Africa. *Presentation at 'ESA Living Planet Symposium 2019', Milan, Italy, 13-17 May 2019*. <https://drive.google.com/file/d/1JOsOYN8XGHVjulEhfTaqFE0S3RpwPgJ/view>

IPBES (2019). Summary for policymakers of the global assessment report on biodiversity and ecosystem services of the Intergovernmental Science-Policy Platform on Biodiversity and Ecosystem Services. S. Díaz, J. Settele, E. S. Brondízio E.S., H. T. Ngo, M. Guèze, J. Agard, A. Arneth, P. Balvanera, K. A. Brauman, S. H. M. Butchart, K. M. A. Chan, L. A. Garibaldi, K. Ichii, J. Liu, S. M. Subramanian, G. F. Midgley, P. Miloslavich, Z. Molnár, D. Obura, A. Pfaff, S. Polasky, A. Purvis, J. Razzaque, B. Reyers, R. Roy Chowdhury, Y. J. Shin, I. J. Visseren-Hamakers, K. J. Willis, and C. N. Zayas (eds.). IPBES secretariat, Bonn, Germany. 56 pages.

Larsen, Y.; Engen, G.; Lauknes, T.R.; Malnes, E.; Høgda, K.A. A generic differential InSAR processing system, with applications to land subsidence and SWE retrieval. *In Proceedings of the ESA FRINGE Workshop 2005, ESA ESRIN, Frascati, Italy, 28 November–2 December 2005.*

Murray, N. J. et al. The role of satellite remote sensing in structured ecosystem risk assessments. *Science of the Total Environment* 619–620, 249–257 (2018).

Murray et al., 2019. The global distribution and trajectory of tidal flats. *Nature Research*, 565(7738): 222-225. Doi:10.1038/s41586-018-0805-8.

Oliver-Cabrera, Talib & Wdowinski, Shimon. (2016). InSAR-Based Mapping of Tidal Inundation Extent and Amplitude in Louisiana Coastal Wetlands. *Remote Sensing*. 8. 393. 10.3390/rs8050393

Pettorelli et al., 2016. Framing the concept of satellite remote sensing essential biodiversity variables: challenges and future directions. *Remote Sensing in Ecology and Conservation*, 2(2): 122-131. Doi: 10.1002/rse2.15.

Rebelo, L.-M., Finlayson, C.M., Strauch, A., Rosenqvist, A., Perennou, C., Tøttrup, C., Hilarides, L., Paganini, M., Wielaard, N., Siegert, F., Ballhorn, U., Navratil, P., Franke, J., and Davidson, N., 2018. The use of Earth Observation for wetland inventory, assessment and monitoring: An information source for the Ramsar Convention on Wetlands. *Ramsar Technical Report No.10. Gland, Switzerland: Ramsar Convention Secretariat.*

Robbi Bishop-Taylor, Stephen Sagar, Leo Lymburner, Robin J. Beaman. Between the tides: Modelling the elevation of Australia's exposed intertidal zone at continental scale. *Estuarine, Coastal and Shelf Science*, Volume 223, 2019, 115-128, ISSN 0272-7714, doi: 10.1016/j.ecss.2019.03.006.

Satellite-based Wetland Observation Service, <https://www.swos-service.eu>

Spinosa, A., Ziemba, A., Saponieri, A., Navarro-Sanchez, V. D., Damiani, L., & El Serafy, G. (2018). Automatic Extraction of Shoreline from Satellite Images: a new approach. *In 2018 IEEE International Workshop on Metrology for the Sea; Learning to Measure Sea Health Parameters (MetroSea)(pp. 33-38). IEEE. DOI: 10.1109/MetroSea.2018.8657864*

Ulander, L. Radiometric slope correction of synthetic aperture radar images. *IEEE Trans. Geosci. Remote Sens.* 1996, 34, 1115–1122, doi:10.1109/36.536527.



NORCE Norwegian Research Centre AS
www.norceresearch.no